Available online at www.sciencedirect.com
ScienceDirect
Dyes and Pigments 75 (2007) 585–605
DYES and PIGMENTS
www.elsevier.com/locate/dyepig

An analysis of the photo-reactivity of monoazo reactive dyes derived from H-acid and related naphthalene sulfonic acids using the PM5 method

Toshio Hihara [a,*], Yasuyo Okada [b], Zenzo Morita [c]

[a] Technical Center, DyStar Japan Ltd., Azuchi-machi 1-7-20, Chuo-ku, Osaka 541-0052, Japan
[b] School of Domestic Science, Otsuma Women's University, Sanban-cho, Chiyoda-ku 102-8357, Japan
[c] Tokyo University of Agriculture and Technology, Koganei, Tokyo 184-8588, Japan

Received 20 February 2006; accepted 15 July 2006
Available online 13 October 2006

Abstract

The reactivities (k_0) of 10 reactive azo dyes derived from H-acid (eight) and related naphthalene sulfonic acids (two) on cellulose films toward singlet oxygen ($^1O_2$) were determined by exposing the dyed films immersed in aerobic Rose Bengal solution to a carbon arc. The k_0 values were analyzed in terms of frontier orbital theory using the semiempirical molecular orbital PM5 method, and were confirmed to correlate to the electrophilic frontier density, $f_r^{(E)}$, at the double bonds with high electron density in HOMO for the predominant tautomers of the dyes on cellulose. The azo–hydrazone tautomerism of the dyes examined was analyzed by calculating the standard heat of formation in the gas phase and water using the PM5 method. The modes of reaction between the azo dyes and $^1O_2$ were the ene and/or the [2 + 2] cycloaddition reaction. The reactivities were expressed as the sum of $f_r^{(E)}$ at the corresponding double bonds. The plots of $\log k_0$ against the sum of $f_r^{(E)}$ for all of the dyes examined yielded a close correlation line, and this was considered to be the molecular descriptor of the reactivity of aromatics against $^1O_2$.

Keywords: Reactive dye; Azo dye; H-acid; PM5 method; Electrophilic frontier density; Singlet oxygen; Ene reaction, [2 + 2] Cycloaddition; QSPR

1. Introduction

The photo-oxidation of azo dyes had been initially explained as an ene reaction between hydrazone tautomers (HTs) and singlet oxygen ($^1O_2$) [1–7]. Molecular orbital (MO) treatment has extended the ene reaction to the reaction between azo tautomers (ATs) and $^1O_2$, resulting in the same end products irrespective of the reaction sites in the two tautomers [8,9]. However, only the photo-oxidation of azo dyes with low light fastness has been demonstrated to obey this mechanism by exposing cellophane dyed with these dyes on immersion in an aerobic aqueous Rose Bengal solution [10–13]. The fading of Pyr-Yellow on cellophane immersed in water is almost completely suppressed in the absence of oxygen and is promoted in aerated deuterium oxide [13], while C.I. Reactive Red 22 and Black 5 on cellophane immersed in water shows reductive fading in the absence of additional substrates under anaerobic conditions [14]. It has been found that the addition of substrates such as sodium DL-mandelate and sodium lactate to the aqueous solution in which cellophane dyed with a reactive dye is immersed promotes the photo-reduction process [15]; a decrease in the concentration of oxygen in the aqueous solution promotes the reduction, while an increase suppresses it [15–17].

* Corresponding author. Tel.: +81 6 6263 6681; fax: +81 6 6263 6697.
E-mail address: hihara.toshio@dystar.com (T. Hihara).

0143-7208/$ - see front matter © 2006 Elsevier Ltd. All rights reserved.
doi:10.1016/j.dyepig.2006.07.007

Although quantitative structure–activity relationships (QSAR) and quantitative structure–property relationships (QSPR) analyzed using MO theory have been widely applied to drug design [18–20], they have rarely been applied to the research and development of dyes. In the field of dyestuff synthesis, colorfastness testing by means of, for example, ISO methods has been carried out to characterize their performance. Unfortunately, no fastness ratings have been found to reflect the essential properties of the dyes themselves, and the colorfastness correlates only indirectly with their properties. Only the absorption spectra have been analyzed by MO methods, but insufficiently [21]. Before applying quantum-mechanical methods to this field, therefore, we must find a way to characterize the dye properties using MO theory and clarify to what degree this can be done. Moreover, those dye properties which can be quantum-mechanically manipulated must be determined experimentally.

From this point of view, the present authors applied frontier orbital theory to analyze the reactivity of azo dyes toward $^1O_2$ and bleaching agents [8,9], in addition to the analysis of the azo–hydrazone tautomerism (AHT) [9,22–25]. These experimental methods have been applied to pyrazolinylazo [23], azobenzene dyes [24] and monoazo dyes derived from γ-acid [25], and it has been shown that the reactivities of these three series of dyes can be quantum-mechanically parameterized. Their reactivities toward $^1O_2$ have been found to be dependent primarily upon the electron densities of HOMO at the carbon atom of the coupling position. This is shown by the large d_{HOMO} value at the acid coupling site of the ATs and the small d_{HOMO} at the carbon atom of the alkaline coupling site of the HTs as well as at the double bonds in the aromatic rings: two fixed double bonds in the pyrazoline ring of pyrazolinylazo dyes [23], the double bonds in the benzene ring of azobenzene dyes which are dependent on the introduced substituents [24], and the double bonds in monoazo dyes derived from γ-acid [25]. These substituents also had the opposite effect of lowering the electron densities or decreasing the reactivity. The modes of reaction with $^1O_2$ at the double bonds were the ene and/or the [2 + 2] cycloaddition reaction. The three series of dyes showed a good correlation between $\log k_0$ and the sum of the electrophilic frontier densities, $f_r^{(E)}$, for the double bonds, but the individual correlations were different among the three series. The sum of $f_r^{(E)}$ is a descriptor of the reactivity in quantum-mechanical QSPR for reactive azo dyes.

In the present paper, the same MO theory and experimental methods as in the previous studies were applied to a series of azo dyes derived from H-acid and related compounds. The investigation of the applicability of these methods as well as of their limitations was another aim of the present study. Since azo dyes derived from H-acid are the greatest group of reactive dyes which give red, blue, navy blue and black, fundamental studies on these dyes are expected to be important for the elucidation of the structure–property relationship of reactive azo dyes. Although no diazo dyes derived from H-acid were examined in this study, the results are expected to lead to further research on the structure–property relationship of diazo dyes.

2. Experimental

2.1. Dyes

Six vinylsulfonyl (VS) and four heterobifunctional reactive dyes derived from H-acid (eight) and related naphthalene sulfonic acids (two) were used. Some of these dyes were the same ones used in the previous study [26]. The chemical structures of the azo tautomers of these dyes are given below, together with the C.I. Generic Names, the abbreviations in parentheses and the C.I. Constitution Numbers, where available:

(1) C.I. Reactive Red 180 (Red 180), C.I. 181055

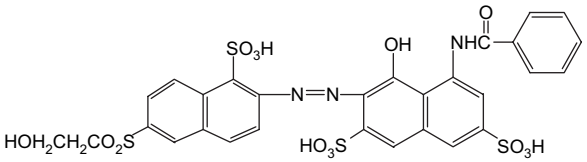

(2) An azo VS dye (Red VST)

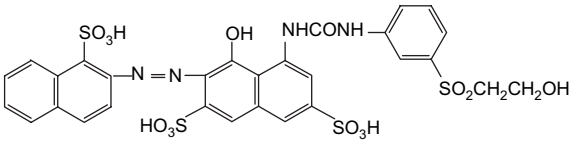

(3) An azo VS dye (Red BR)

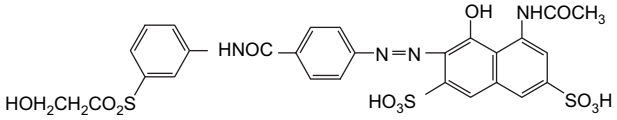

(4) An azo VS dye (Red VSK)

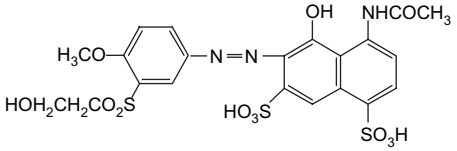

(5) An azo VS dye (Red VSP)

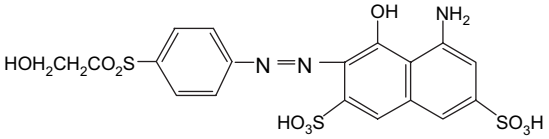

(6) C.I. Reactive Red 194 (Red 194), C.I. 18214

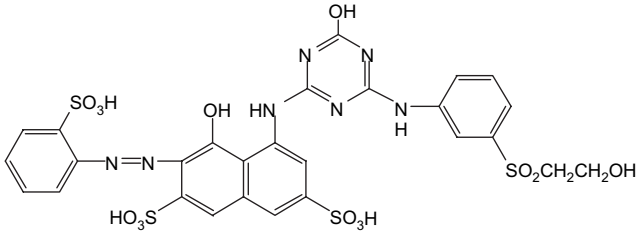

(7) C.I. Reactive Red 227 (Red 227), C.I. 18215

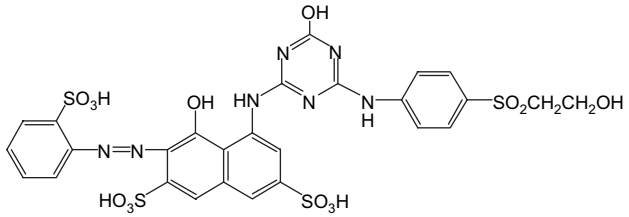

(8) C.I. Reactive Red 241 (Red 241), C.I. 18220

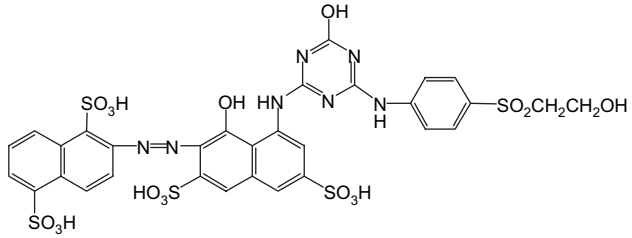

(9) C.I. Reactive Red 198 (Red 198), C.I. 18221)

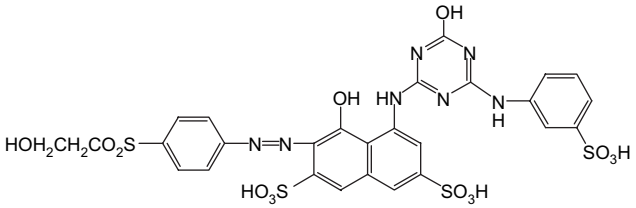

(10) A Red VS dye derived from naphthionic acid (Congo VS)

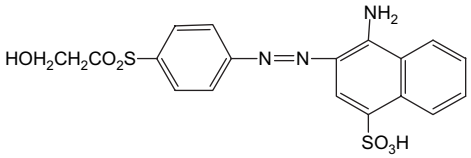

(11) An aminopyrazolinyl azo dye (Pyr-Yellow)

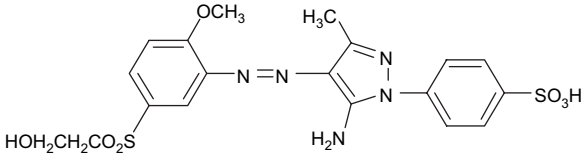

2.2. Semiempirical molecular orbital calculation using the PM5 method

All the MO calculations were carried out using CAChe MOPAC 2002 (Windows edition, version 6.1.12.33) (Fujitsu, Ltd.) [27]. This version gave different results for some azo dyes containing a triazine ring from those given by the previous version. The parameters of the COSMO method were also modified (van der Waals radius of water = 0.13 nm). For the ATs and HTs of the 10 dyes in the gas phase and water, structure optimization was performed to obtain their molecular parameters such as the standard heat of formation, $\Delta_f H^0$(gas) and $\Delta_f H^0(H_2O)$ (kcal mol^{-1}), in the gas phase and water, the energies of HOMO and LUMO, E_{HOMO} and E_{LUMO}, the electron densities in HOMO, d_{HOMO}, the electrophilic frontier densities, $f_r^{(E)}$, and the dipole moment, μ, in the gas phase using the PM5 method. The COSMO method was used to calculate the parameters in water. The $\Delta_f H^0$(gas) values were also estimated for the reaction intermediates of the corresponding tautomers at the transition-state geometry (TSG). Structural optimization was carried out to calculate the $\Delta_f H^0$(gas) values for the reaction intermediates and products at the PM5 geometry.

2.3. Photo-sensitised oxidative fading on cellulose films

In order to minimize the self-photosensitization effect of the red dyes examined, cellophane film was dyed using the same method as before [28] and the absorbance of red dyes at λ_{max} on a sheet of cellulose film was brought to approximately 0.3–0.4, since no filter could be used due to the superposition of the absorption spectra of Rose Bengal on those of the red dyes. The same method of exposure was applied to determine the relative fading [23–25].

3. Results and discussion

3.1. The ease with which dyes are photo-oxidized and their photosensitivity

The second-order rate constants, k_0 (mol^{-1} dm^3 s^{-1}), of the 10 dyes for the reaction against $^1O_2$ promoted by photosensitization with Rose Bengal were estimated from the fading profiles of the dyes. In our previous study, they were determined based on the relative fading upon exposure for 5 h [26], while in the present study, the k_0 values were determined based on the initial rate of the relative fading, as in other previous studies [23–25].

Since the proportion of dye molecules in the excited states is low and the lifetime is very short, dye molecules in the ground state can become oxidized. The oxidation of dye molecules is controlled not only by the second-order kinetic equation but also by the quantum yield of singlet oxygen generation. Assuming the steady state of generation for $^1O_2$, or using Pyr-Yellow as the reference, whose k_0 value was estimated on the basis of the same assumption [28], the k_0 values for the 10 dyes were determined, as listed in Table 1.

3.2. The photo-decomposed products of red azo dyes bound with cellulose

In a series of studies in which the photodecomposition of reactive dyes on cellulose was analyzed, the authors [13–17] reported that the absorption spectra of the decomposed

Table 1
Values of the rate constant, k_0 ($dm^3\ mol^{-1}\ s^{-1}$), of the second-order reaction with $^1O_2$ estimated from the initial slope of relative fading, A/A_0, for red and yellow reactive dyes on cellulose immersed in aerated Rose Bengal (3.3×10^{-5} M + 0.5 M Na_2SO_4) solution on exposure to carbon arc without filter, and the observation of the absorption spectra of decomposition products attached to cellulose

No	Dye	k_0	Symbol for Fig. 6	Absorption spectra of decomposed products on cellulose
1	Red 180[a]	0.14	180	AS of 1-sulfo-6-(2-hydroxyethylsulfonyl)naphthol
2	Red 198	0.15_0	198	A mixture of AS nearly similar to the DP of Red 194 group and AS nearly similar to the DP of Yellow VST
3	Red 194[a]	0.46	194	AS similar to Red 227 and 241
4	Red 227[a]	0.28	227	AS similar to Red 194 and 241
5	Red 241[a]	0.17	241	AS similar to Red 194 and 227
6	Red VST	0.64_9	T	Only particular spectra
7	Red BR	0.45_4	BR	AS similar to Red VSK
8	Red VSK	0.60_4	K	3-(2-hydroxyethylsulfonyl)-4-methoxyphenol
9	Red VSP	2.6_1	P	4-(2-hydroxyethylsulfonyl)phenol
10	Congo VS	3.0_0	CV	AS similar to Red VSP
11	Pyr-Yellow	6.9 [11]	–	AS similar to Yellow 14 and Red 22

AS = absorption spectra, DP = double peaks.
[a] C.I. reactive generic name.

products indicated the existence of residues of reactive anchors attached to the cellulose substrate as well as the existence of decomposed fragments of chromophores in cases where the fragments were bound with the anchors. The absorption spectra of the exposed samples for the 10 dyes examined in this study will be discussed based on the spectral analysis results (cf. Figs. 1–5). The patterns of the absorption

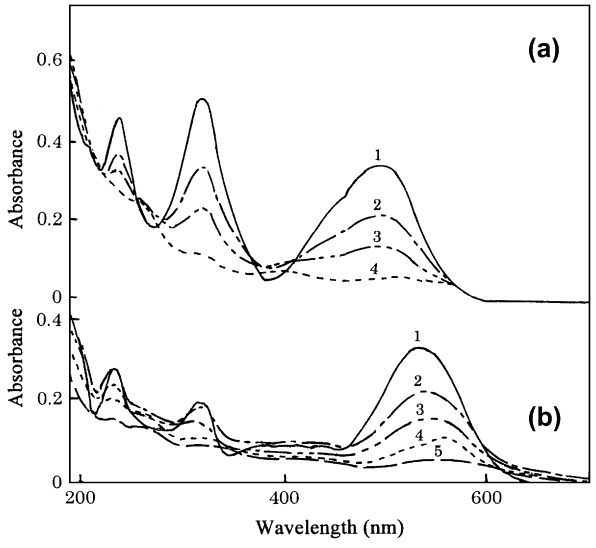

Fig. 1. The absorption spectra of (a) Congo VS and (b) Red VSP of the original (1) and of the decomposed products on cellophane film immersed in Rose Bengal solution after exposure to a carbon arc. Exposure times: 15 min (2), 30 min (3) and 60 min (4); the calculated spectrum (5) of the decomposed products. (It was obtained by subtracting the original spectrum of Red VSP (4) at the corresponding concentration from that of the exposed sample. No calculated spectrum is shown for Congo VS.)

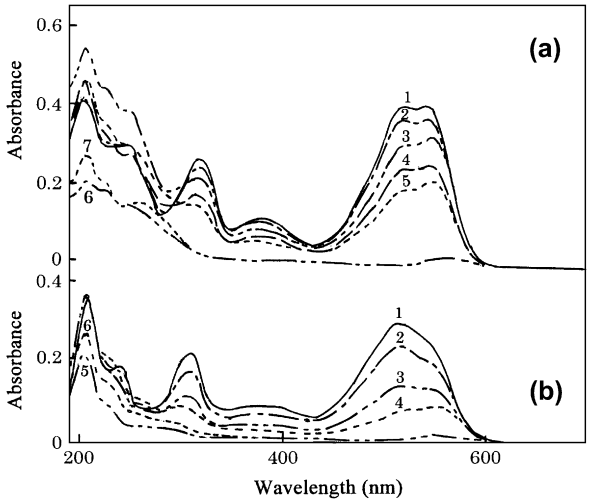

Fig. 2. The absorption spectra of (a) Red BR and (b) Red VSK of the original (1) and of the decomposed products on cellophane film immersed in Rose Bengal solution after exposure to a carbon arc. Exposure times for Red BR (a): 30 min (2), 2.5 h (3), 5 h (4) and 10 h (5); the calculated spectra (6 and 7) of the decomposed products for Red BR. (They were obtained by subtracting the original spectrum of Red BR (1) at the corresponding concentration from those (spectra 3 and 5) of exposed samples, respectively.) Exposure times for Red VSK (b): 30 min (2), 1 h (3) and 5 h (4); the calculated spectra (5 and 6) of the decomposed products for Red VSK. (They were obtained by subtracting the original spectrum of Red VSK (1) at the corresponding concentration from those (spectra 3 and 4) of the exposed samples, respectively.)

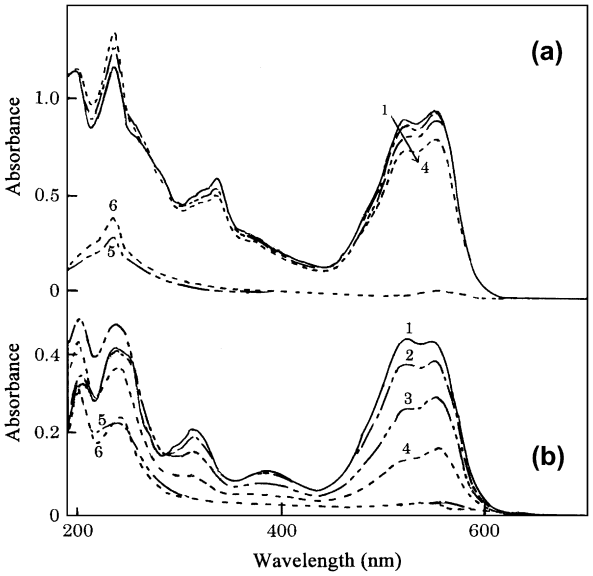

Fig. 3. The absorption spectra of (a) Red 180 and (b) Red VST of the original (1) and of the decomposed products on cellophane film immersed in Rose Bengal solution after exposure to a carbon arc. Exposure times for Red 180 (a): 1 h (2), 5 h (3) and 10 h (4); the calculated spectra (5 and 6) of the decomposed products for Red 180. (They were obtained by subtracting the original spectrum of Red 180 (1) at the corresponding concentration from those (spectra 3 and 4) of exposed samples, respectively.) Exposure times for Red VST (b): 30 min (2), 2.5 h (3) and 10 h (4); the calculated spectra (5 and 6) of the decomposed products for Red VST. (They were obtained by subtracting the original spectrum of Red VST (1) at the corresponding concentration from those (spectra 3 and 4) of the exposed samples, respectively.)

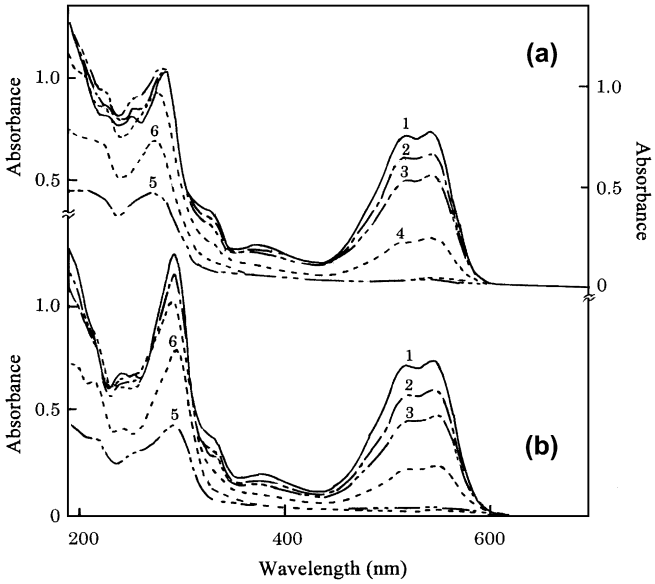

Fig. 4. The absorption spectra of (a) Red 194 and (b) Red 227 of the original (1) and of the decomposed products on cellophane film immersed in Rose Bengal solution after exposure to a carbon arc. Exposure times for Red 194 (a): 1 h (2), 2.5 h (3) and 10 h (4); the calculated spectra (5 and 6) of the decomposed products for Red 194. (They were obtained by subtracting the original spectrum of Red 194 (1) at the corresponding concentration from those (spectra 3 and 4) of the exposed samples, respectively.) Exposure times for Red 227 (b): 1 h (2), 2.5 h (3) and 10 h (4); the calculated spectra (5 and 6) of the decomposed products for Red 227. (They were obtained by subtracting the original spectrum of Red 227 (1) at the corresponding concentration from those (spectra 3 and 4) of the exposed samples, respectively.)

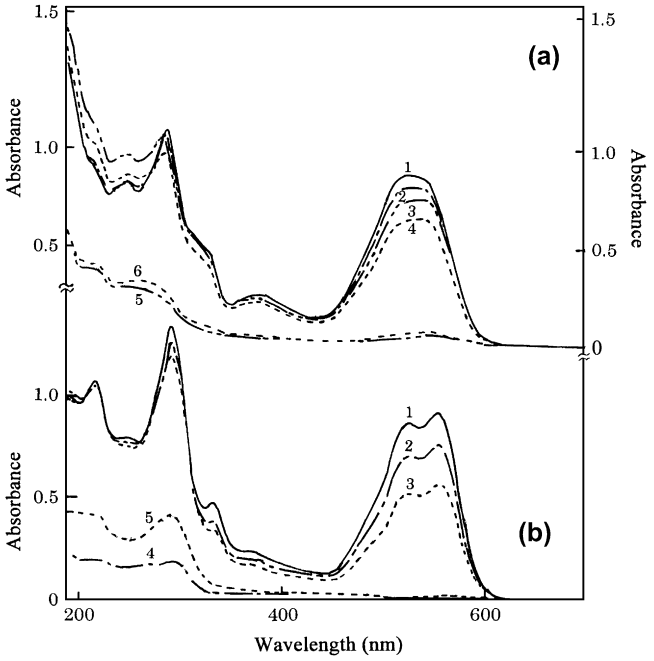

Fig. 5. The absorption spectra of (a) Red 198 and (b) Red 241 of the original (1) and of the decomposed products on cellophane film immersed in Rose Bengal solution after exposure to a carbon arc. Exposure times for Red 198 (a): 1 h (2), 5 h (3) and 10 h (4) the calculated spectra (5) of the decomposed products for Red 198. (They were obtained by subtracting the original spectrum of Red 198 (1) at the corresponding concentration from those (spectra 3 and 4) of exposed samples, respectively.) Exposure times for Red 241 (b): 2.5 h (2) and 10 h (3); the calculated spectra (4 and 5) of the decomposed products for Red 241. (They were obtained by subtracting the original spectrum of Red 241 (1) at the corresponding concentration from those (spectra 2 and 3) of the exposed samples, respectively.)

spectra of the decomposed products bound with cellulose were classified under several groups of reactive anchors, as summarized in Table 1. The reaction schemes for the reactions with $^1O_2$ are discussed in Section 3.3.

3.2.1. The absorption spectra of the decomposed products of azo dyes with a VS or MCT anchor in the diazo component

3.2.1.1. Group A (azo dyes derived from the vinylsulfonylaniline derivative (diazo component) anchor). The diazo components used are classified as follows:

(1) 4-vinylsulfonylaniline (Red VSP and Congo VS)
(2) vinylsulfonyl-4-methoxyaniline (Red VSK)
(3) 4-(3-vinylsulfonylphenyliminocarbonyl)aniline (Red BR)
(4) 1-sulfo-6-vinylsulfonyl-2-naphthylamine (Red 180)

As reported in some of our previous papers [23–25], the absorption spectra of Group A exhibited very clearly the structural change in the diazo component bound with cellulose through a VS anchor.

3.2.2. Azo dyes with a VS anchor in the coupling component

3.2.2.1. Group B (azo dyes derived from H-acid with an N-substituted phenyl group with a VS anchor). Red VST belongs to this group. *m*-VS-phenyl-ureido-substituted naphthol sulfonic acid undergoes primarily the ene and/or the [2 + 2] cycloaddition reaction at the coupling position. Since the naphthalene nucleus may suffer oxidative attack at various sites, the absorption spectra of a mixture of naphthalene residues with carbonyl fragments generated by thermal and/or photo-decomposition can be observed.

3.2.2.2. Group C (azo dyes derived from H-acid with a substituted triazinyl group). Red 194, Red 227 and Red 241 (*N*-2-vinylsulfonylanilino-4-hydroxytriazinyl-H-acid), also called mixed bifunctional reactive dyes, belong to this group. They show spectra similar to that of Red VST, since they are Red VST with the triazinyl group substituted by a benzoyl group. The triazine ring may cover the reaction which occurs in the chromophore.

3.2.3. Azo dyes with a VS anchor in the diazo component and an MCT anchor in the coupling component

3.2.3.1. Group D (azo dyes derived from H-acid with a substituted triazinyl group). Red 198 belongs to this group. Since both the VS and the MCT anchor always bind with cellulose, the absorption spectra of the decomposed products may depend upon the state of the dye–cellulose binding if azo scission occurs via the decomposition. The spectra, therefore, may

give no proof of the reaction, even if they can be completely elucidated.

3.3. The AHT of reactive red dyes

The values of $\Delta_f H^0$(gas) and $\Delta_f H^0(H_2O)$ for the 10 dyes were calculated using the PM5 method, as listed in Tables 2 and 3. The λ_{max} of the azo dyes shifts from water through organic solvents to dry cellulose in parallel with the dielectric constant. Dry cellulose may be regarded as a medium closer to the gas phase due to the low dielectric constant. So, cellulose may have an intermediate solvation effect, between that of water and that of the gas phase. When a dye exists as the same tautomer in these two latter phases, the dye may be said to exist as the same tautomer on cellulose as well; if it exists as different tautomers in the gas phase and water, it exists on cellulose as one of the two tautomers. Since no shift in the λ_{max} value of the azo dyes was noticed on cellulose upon swelling in water, it may be assumed that the swelling caused by water has no effect on the solvation of these dyes on cellulose.

Compared with the AHT of the series of dyes examined previously [22–26], the differences in the $\Delta_f H^0$ values in the present series were small between the tautomers in the gas phase and water, and the AHT changes were complex, no regularity being found. This may be attributed to the relatively small changes in the $\Delta_f H^0$ values caused by the AHT changes, compared with the $\Delta_f H^0$ values for large dye molecules (molecular weight > 600), because AHT changes occur only around the azo groups.

3.4. The reactivity of azo dyes undergoing photo-sensitised oxygenation in terms of frontier orbital theory

Among the chemical reactions between $^1O_2$ and the predominant tautomers of azo dyes existing on water-swollen cellulose, the reactions yielding (1) dioxetans or carbonyl fragments via [2 + 2] cycloaddition (dioxetane reaction) and (2) allylic hydroperoxides via 1,3-addition (ene reaction) have been reported to contribute to oxidative decomposition [22–25]. In this study, the reactivity, i.e. the reaction modes, the sites of reaction, and the reaction rates (k_0) were analyzed in terms of $f_r^{(E)}$ by determining the correlation between log k_0 and the sum of the $f_r^{(E)}$ values, $S_{m,n}^{(E)}$.

Let us first explain these two parameters. A quantity called the frontier electron density, which is the weighted sum of the squares of the coefficients of LCAO MO, has been introduced by Fukui et al. [29]. The sum is weighted by the difference in energy from that of the frontier orbital (HOMO, in the case of electrophilic reactions). Fukui's original expression for electrophilic reactions can be expressed as follows:

$$f_r^{(E)} = \frac{\sum_{j=1}^{N} \nu_j \left(C_r^j\right)^2 \exp\left\{-\lambda\left(E_{HOMO} - E_j\right)\right\}}{\sum_{j=1}^{N} \nu_j \exp\left\{-\lambda\left(E_{HOMO} - E_j\right)\right\}} \quad (1)$$

In this equation, the superscript (E) is the electrophilic reaction, and the subscript r is the atomic position. N is the total number of orbitals, ν_j is the number of electrons in the jth orbital

Table 2
Enthalpy of formation, $\Delta_f H^0$ (kcal mol^{-1}), HOMO and LUMO energies, E_{HOMO} and E_{LUMO} (eV), and electron density of HOMO and LUMO, d_{HOMO} and d_{LUMO}, at given atoms for azo and hydrazone tautomers of azo dyes with a VS anchor, derived from H-acid and other naphthalene sulfonic acid in the gas phase, estimated by semiempirical molecular orbital PM5 method

	Red 180		Red VST		Red BR		Red VSK		Congo VS	
M.W.	765.752		780.767		692.686		603.590		435.469	
	AT	HT	AT	HT	AT	HT	AT	HT	AT	HT
$\Delta_f H^0$(gas)	−404.838	−406.375	−405.440	−403.003	−350.396	−352.396	−371.664	−373.428	−133.392	−123.388
μ	6.538	11.774	11.954	8.580	9.533	7.600	6.309	5.283	5.790	6.727
E_{HOMO}	−9.644	−9.861	−9.815	−9.548	−9.587	−9.455	−9.330	−9.876	−9.123	−9.263
E_{LUMO}	−2.599	−3.063	−2.583	−2.799	−2.546	−2.740	−2.195	−2.449	−1.744	−2.020
$\Delta_f H^0(H_2O)$	−479.217	−482.347	−478.950	−476.124	−423.393	−425.365	−432.410	−432.929	−172.845	−165.090
$f_r^{(E)}$ (Position) for the most probable tautomer	HT		AT		HT		HT		AT	
	0.060 (C13)		0.077 (C1)		0.203 (C1)		0.251 (C13)		0.377 (C1)	
	0.184 (C22)		0.081 (C2)		0.041 (N11)		0.087 (C14)		0.073 (C2)	
	0.078 (C17)		0.083 (C4)		0.075 (C18)		0.124 (C16)		0.092 (C4)	
	0.109 (C18)		0.049 (C5)		0.081 (C13)		0.141 (C17)		0.121 (C5)	
			0.130 (C27)		0.061 (C14)		0.105 (C15)		0.035 (C13)	
			0.049 (C28)		0.073 (C9)				0.045 (C14)	
	0.076 (C1)		0.043 (C29)		0.058 (C10)				0.063 (C3)	
	0.031 (N11)		0.110 (C30)		0.043 (C4)		0.053 (C9)		0.033 (C8)	
	0.034 (C4)		0.035 (C31)		0.054 (C5)		0.044 (C10)			
	0.041 (C5)		0.093 (C32)				0.023 (C18)			
	0.029 (C9)						0.022 (C4)		0.025 (C6)	
	0.041 (C10)		0.049 (C9)		0.008 (C3)		0.066 (C5)		0.137 (C7)	
			0.034 (C10)		0.020 (C8)		0.032 (C3)		0.040 (N11)	
	0.011 (C3)		0.020 (C6)		0.029 (C15)		0.013 (C8)		0.183 (N12)	
	0.023 (C8)		0.043 (C7)		0.101 (C16)		0.147 (C1)			
			0.028 (N11)		0.016 (C17)		0.073 (N11)			
			0.045 (N12)							

Table 3
Enthalpy of formation, $\Delta_f H$ (kcal mol^{-1}), HOMO and LUMO energies, E_{HOMO} and E_{LUMO} (eV), electron density of HOMO and LUMO, d_{HOMO} and d_{LUMO}, at given atoms for azo and hydrazone tautomers of heterobifunctional reactive monoazo dyes derived from H-acid and of a model dye in the gas phase, estimated by semiempirical molecular orbital PM5 method

	Red 194		Red 227		Red 241		Red 198		Red VSP	
M.W.	765.752		797.757		927.875		797.757		531.526	
	AT	HT	AT	HT	AT	HT	AT	HT	AT	HT
$\Delta_f H^0$ (gas)	−391.468	−390.746	−390.261	−389.799	−481.671	−481.223	−388.407	−389.314	−291.469	−294.842
μ	6.575	8.870	3.899	8.294	6.761	6.232	7.534	10.106	4.022	6.097
E_{HOMO}	−9.477	−9.849	−9.456	−9.905	−9.810	−9.775	−9.592	−9.264	−9.261	−9.279
E_{LUMO}	−2.399	−2.302	−2.416	−2.443	−2.797	−2.874	−2.475	−2.668	−2.521	−2.695
$\Delta_f H^0$ (H_2O)	−460.568	−462.804	−461.585	−466.395	−570.876	−568.868	−464.750	−466.440	−348.675	−354.223
$f_r^{(E)}$ (X)	AT	HT	AT	HT	AT	HT	HT		HT	
	0.191 (C1)	0.145 (C28)	0.180 (C1)	0.069 (C28)	0.114 (C1)	0.103 (C1)	0.111 (C9)		0.215 (C1)	
	0.159 (C2)	0.104 (C29)	0.153 (C2)	0.077 (C29)	0.096 (C2)	0.041 (N11)	0.067 (C10)		0.048 (N11)	
	0.105 (C9)	0.044 (C30)	0.096 (C9)	0.102 (C33)	0.101 (C4)	0.063 (C16)	0.117 (C14)		0.078 (C4)	
	0.054 (C10)	0.115 (C31)	0.047 (C10)	0.035 (C30)	0.071 (C5)	0.056 (C21)	0.074 (C13)		0.163 (C5)	
	0.141 (C4)	0.047 (C32)	0.059 (C13)	0.107 (C31)	0.067 (C9)	0.049 (C14)	0.108 (C18)		0.074 (C14)	
	0.098 (C5)	0.061 (C33)	0.062 (C18)		0.044 (C10)	0.033 (C13)			0.054 (C13)	
	0.058 (C18)		0.037 (C15)			0.062 (C22)			0.092 (C18)	
	0.054 (C13)	0.049 (C3)	0.065 (C16)			0.041 (C9)	0.043 (C4)		0.072 (C9)	
		0.046 (C8)	0.031 (C6)		0.029 (C14)	0.054 (C10)	0.051 (C5)		0.069 (C10)	
	0.033 (C15)		0.082 (C7)		0.031 (C13)	0.042 (C4)	0.333 (C1)		0.073 (C3)	
	0.059 (C16)		0.137 (C4)		0.033 (C22)	0.052 (C5)	0.031 (N11)		0.041 (C8)	
	0.021 (C14)		0.098 (C5)		0.039 (C16)		0.010 (C3)			
	0.035 (N11)				0.035 (C21)		0.018 (C8)			
	0.088 (N12)		0.036 (N11)		0.019 (N11)	0.029 (C8)			0.348 (N12)	
	0.012 (C3)		0.082 (N12)		0.052 (N12)	0.013 (C3)				
	0.011 (C8)		0.012 (C3)		0.009 (C8)					
	0.031 (C6)		0.010 (C8)		0.009 (C3)					
	0.084 (C7)		0.023 (C14)							

(usually 0, 1, or 2), C_r^j is the coefficient of the jth LCAO MO at the rth atomic position, E_j is the energy of the jth orbital, and λ is a scale factor (usually set to 3.0 in these calculations) [27].

The electrophilic reactivity of the double bonds toward $^1O_2$ is described by the sum, $S_{m,n}^{(E)}$, of the reactivities of the two atomic positions, as follows:

$$S_{m,n}^{(E)} = \sum_{m,n} \{f_m^{(E)} + f_n^{(E)}\} \quad (2)$$

where m and n denote the neighboring atomic positions of the corresponding double bonds; when these positions overlap, the overlapping position is counted only once. Double bonds with larger values of $(f_m^{(E)} + f_n^{(E)})$ are taken into consideration one by one. $^1O_2$ has no reactivity toward isolated atomic positions with larger $f_r^{(E)}$ values, such as nitrogen imino bridge groups and the oxygen in sulfonate groups. The summation of Eq. (2) is valid from the position with the largest value of $(f_m^{(E)} + f_n^{(E)})$ to the site of reaction limit. The $S_{m,n}^{(E)}$ values may describe the reactivity of a dye against $^1O_2$, a molecular descriptor for the ene and/or the [2 + 2] cycloaddition reaction.

In order to confirm whether or not these MO theories can be applied to the ene and/or the [2 + 2] cycloaddition reactions of the ATs and HTs with $^1O_2$, the $S_{m,n}^{(E)}$ values defined by Eq. (2) were plotted against the logarithmic k_0 values determined experimentally (cf. Fig. 6). The possible reaction modes and their primary positions are summarized in Table 4. Taking all of the possibilities into consideration, the positions along the ordinate were determined or fixed experimentally, while those along the abscissa were determined so as to extract a general correlation between the logarithmic k_0 values and the $S_{m,n}^{(E)}$ values. The course of analysis for individual dyes is explained next.

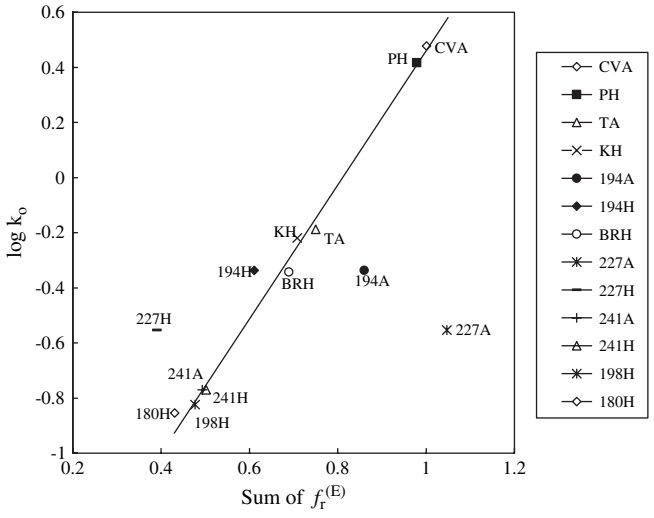

Fig. 6. The relationship between log k_0 and the sum of $f_r^{(E)}$ for the series of azo dyes derived from H-acid examined in this study. The symbols in the figure are described in Table 1 and those signifying the tautomers ("A" for ATs and "H" for HTs) are added to the dye symbols.

Table 4
Azo–hydrazone tautomerism of azo dyes derived from H-acid and their related naphthalene sulfonic acids and probable mode of reaction with $^1O_2$ (cf. Tables 2, 3, 5–7)

No.	Red dyes	Tautomer (phase)	Ene (site)	[2 + 2] Addition			
			In common	In common	Uniquely		
1	Red VST	AT(g&w)	C1=C2; H (O23)	C1=C2, C4=C5	C27=C28, C29=C30, C31=C32		
2	Congo VS				C3=C8, C13=C14		
3	Red BR	HT(g&w)					
4	Red VSP		C1=N11; H (N12)	C1=N11, C4=C5, C9=C10, C13=C14, C13=C18	C3=C8		
5	Red VSK				C13=C14, C15=C16, C16=C17		
6	Red 180[a]				C13=C22, C17=C18		
7	Red 198[a]				C9=C10, C13=C14, C13=C18		
		Tautomer (phase)	Ene (site)		[2 + 2] Addition		
			AT	HT	In common	AT	HT
8	Red 194[a]	AT(g) → HT(w)	C1=C2; H(O23)			C1=C2, C4=C5, C9=C10, C13=C18	C3=C8, C28=C29, C30=C31, C32=C33
9	Red 227[a]	AT/HT(g) → AT(w)				C1=C2, C4=C5, C6=C7, C9=C10, C13=C18, C15=C16	C28=C29, C30=C31, C28=C33
10	Red 241[a]	AT/HT(g) → HT(w)		C1=N11; H(N12)	C4=C5, C9=C10	C1=C2	C1=N11, C13=C14, C13=C22, C16=C21

[a] C.I. reactive generic name.

3.5. The reaction modes of the ATs and HTs of azo dyes on cellulose film

3.5.1. The ATs of an azo dye, Congo VS, derived from naphthionic acid

As a prototype of the reactivity of azo dyes derived from naphthalene sulfonic acid, Congo VS was examined. The name "Congo VS" stems from Congo Red (C.I. Direct Red 1), since the former has half the structure of the latter. The values of $\Delta_f H^0$(gas) and $\Delta_f H^0(H_2O)$ (cf. Table 2) indicate that this dye exists as ATs in both the gas phase and water as well as on cellulose.

As in the previous papers [23–25], the double bonds with higher reactivities against $^1O_2$ can be selected from the d_{HOMO} listed in Table 5. The double bonds with possible reactivity are C1=C2, C3=C8, C4=C5, C13=C14 and C6=C7. The double bond C3=C8 cannot be excluded in spite of the small value of d_{HOMO} at C8 (0.008, the lower limit of reactivity), while the double bond C6=C7 may be excluded due to the small value of $f_r^{(E)}$ at C6 (0.025), which lies below the lower limit of reactivity. As in the previous studies, the $\Delta_f H^0$(gas) values of the reaction intermediates and products for each mode were calculated using the PM5 method (cf. Tables 8–10). The double bond N11=N12 can be excluded due to the very small value of d_{HOMO} (0.002) at N11 as well as the very large energy barrier for forming hydroperoxide (cf. Table 10 and order (3)) [23–25]. Since the $\Delta_f H^0$(gas) values for the reaction intermediates were similar, no comparison between the modes was possible. The order of reactivity based on the $\Delta_f H^0$(gas) values of the reaction products is as follows:

$$\begin{aligned}&\text{ene(C1=C2; H(O19))} > \text{[2 + 2]addition(C4=C5)}\\ &> \text{[2 + 2]addition(C6=C7)} > \text{[2 + 2]addition(C1=C2)}\\ &> \text{[2 + 2]addition(C13=C14)} > \text{[2 + 2]addition(C3=C8)}\\ &\gg \text{[2 + 2]addition(N11=N12).}\end{aligned} \quad (3)$$

No calculation of $\Delta_f H^0$(gas) for the reaction product of [2 + 2] addition (C13=C18) was carried out because of the symmetrical identity between C13=C14 and C13=C18. Although no $S_{m,n}^{(E)}$ values could be used to discriminate between ene and [2 + 2] addition, the reactivities in order (3) and those based on the $S_{m,n}^{(E)}$ values coincided with each other, and this fact may indicate that the ene reactivity was higher than the [2 + 2] addition reactivity at C1=C2.

In Tables 8–10, the $\Delta_f H^0$(gas) values for the HTs of the reaction intermediates and products of each mode are also listed. They were smaller than those for the ATs in all cases. This fact indicates that Congo VS may exist as ATs during the reaction.

The plot of $S_{m,n}^{(E)}$ $(m,n$: 1, 2; 4, 5; 3, 8; 13, 14) against $\log k_0$ may be used to determine the reaction point for this dye. As mentioned below, after the plots of the other dyes were added, the plot of this dye coincided with the common correlation line (Fig. 6).

The reaction schemes and the absorption spectra of the photodecomposed products are discussed below (Section 3.5.2.1).

Table 5
Electron densities, d_{HOMO}, at each atom for the A&HTs of C.I. Reactive Red 180 and its related compounds in the gas phase, using PM5 method

Dye	Red 180[a]		Red VST[b]			Red VSP[c]		Congo VS[d]	
Tautomer	AT d_{HOMO}	HT d_{HOMO}	AT d_{HOMO}	HT d_{HOMO}		AT d_{HOMO}	HT d_{HOMO}	AT d_{HOMO}	HT d_{HOMO}
C1	0.175	0.071	0.023	0.108	C1	0.109	0.121	0.215	0.140
C2	0.110	0.000	0.025	0.000	C2	0.065	0.001	0.042	0.001
C3	0.001	0.000	0.000	0.000	C3	0.016	0.024	0.022	0.020
C4	0.102	0.014	0.031	0.021	C4	0.106	0.040	0.051	0.007
C5	0.088	0.019	0.018	0.028	C5	0.157	0.087	0.059	0.035
C6	0.023	0.000	0.006	0.000	C6	0.025	0.002	0.008	0.002
C7	0.075	0.021	0.016	0.029	C7	0.123	0.107	0.076	0.022
C8	0.001	0.009	0.000	0.009	C8	0.002	0.020	0.008	0.029
C9	0.099	0.025	0.015	0.039	C9	0.057	0.041	0.211	0.076
C10	0.050	0.028	0.010	0.032	C10	0.027	0.041	0.004	0.012
N11	0.001	0.024	0.001	0.024	N11	0.001	0.027	0.002	0.032
N12	0.060	0.187	0.006	0.181	N12	0.032	0.195	0.085	0.273
C13	0.004	0.056	0.000	0.050	C13	0.006	0.025	0.010	0.042
C14	0.006	0.011	0.000	0.017	C14	0.006	0.034	0.016	0.067
C15	0.000	0.021	0.000	0.009	C15	0.000	0.002	0.000	0.002
C16	0.007	0.048	0.000	0.059	C16	0.009	0.050	0.018	0.100
C17	0.000	0.026	0.000	0.029	C17	0.000	0.000	0.000	0.000
C18	0.005	0.101	0.000	0.088	C18	0.007	0.042	0.015	0.075
C19	0.000	0.004	0.000	0.002	X19	0.032	0.007	0.143	0.043
C20	0.000	0.081	0.000	0.033	Y20	0.191	0.111	–	–
C21	0.003	0.031	0.000	0.066					
C22	0.008	0.162	0.000	0.066					
O23	0.082	0.009	0.010	0.020					
N24	0.054	0.011	0.006	0.020					
C27	–	–	0.173	0.005					
C28	–	–	0.051	0.003					
C29	–	–	0.039	0.000					
C30	–	–	0.146	0.004					
C31	–	–	0.026	0.000					
C32	–	–	0.114	0.005					

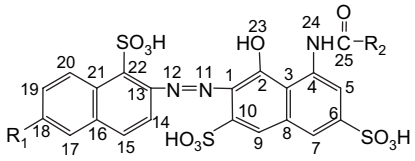

[a] Red 180 ($R_1 = SO_2CH_2CH_2OH$, R_2 = phenyl).

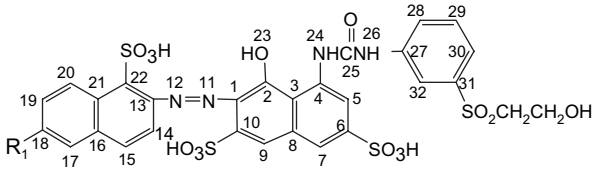

[b] Red VST ($R_1 = H$).

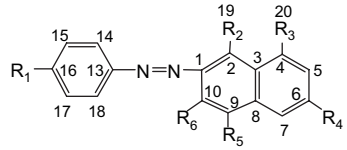

[c] Red VSP ($R_1 = SO_2CH_2CH_2OH$, $R_2 = OH$ (X = O), $R_3 = NH_2$ (Y = N), $R_4 = R_6 = SO_3H$, $R_5 = H$).
[d] Congo VS ($R_1 = SO_2CH_2CH_2OH$, $R_2 = NH_2$ (X = N), $R_3 = R_4 = R_6 = H$, $R_5 = SO_3H$.

3.5.2. The HTs of Red VSP

As another prototype of the reactivity of azo dyes derived from H-acid, Red VSP was examined. The values of $\Delta_f H^0$(gas) and $\Delta_f H^0(H_2O)$ suggested that this dye exists as HTs in the gas phase and water (cf. Table 3). The values of d_{HOMO} shown in Table 5 indicate that the double bonds with possible reactivity are C1═N11, C4═C5, C9═C10, C13═C14, and C13═C18. As in the case of Congo VS, the order of reactivity based on the $\Delta_f H^0$(gas) values of the reaction products (cf. Tables 8–10) is as follows:

$$\begin{aligned}&\text{ene(C1=N11; H(N12))} > \text{[2 + 2]addition(C9=C10)}\\ &> \text{[2 + 2]addition(C4=C5)} > \text{[2 + 2]addition(C13=C14)}\\ &\approx \text{[2 + 2]addition(C13=C18)} > \text{[2 + 2]addition(C14=C15)}\\ &> \text{[2 + 2]addition(C3=C8)} \approx \text{[2 + 2]addition(C1=N11).}\end{aligned} \quad (4)$$

All double bonds mentioned seem to have some reactivity, that is, none of the double bonds can be excluded for any reason. The order of reactivity based on the $S^{(E)}_{m,n}$ values, as listed in Table 3, coincided with order (4). The plot of $S^{(E)}_{m,n}$ (m, n: 1, 11; 3, 8; 4, 5; 14, 13, 18; 9, 10) against log k_0 may be used to determine the reaction point for this dye (Fig. 6). Almost all of the double bonds in Red VSP were found to possess high reactivity.

The $\Delta_f H^0$(gas) values for the ATs of the reaction intermediates and products of each mode were also calculated (cf. Tables 8–10). The values for the HTs were smaller than those for the ATs, except in the case of [2 + 2] addition (C9=C10). This fact indicates that this dye undergoes AHT during the reaction.

3.5.2.1. The relationship between the reaction schemes and the absorption spectra of the decomposed products for Congo VS and Red VSP. The double bonds with the highest reactivity toward $^1O_2$ are C1=C2 for the ATs of Congo VS and C1=N11 for the HTs of Red VSP. If $^1O_2$ were to attack only these two double bonds, the reaction products of these two dyes would be the same irrespective of the reaction mode, as shown in Scheme 1(a) and in the previous papers [23–25]. However, since the other double bonds were attacked by $^1O_2$ as well, a mixture of reaction products was generated, although the behaviors of these products were too complex to analyze in detail. Thus, the absorption spectra of the decomposed products of the two dyes (Fig. 1(a) and (b)) exhibited the same behaviors as those of the decomposition products of monoazo dyes derived from γ-acid with a *p*-VS-type anchor [26]; the increase of base line in the visible region and the resemblance in the pattern of the spectra and the positions of the shoulder in the UV region indicate similar reaction modes, as expected from the reaction mechanism.

As for the reaction mechanism, two atomic positions attached to the azo groups of the two dyes possessed high reactivity. When ene and/or the [2 + 2] addition reactions between $^1O_2$ and C1=C2, C13=C14 or C13=C18 in Congo VS occurred, decoloration or a rapid decrease in the main visible absorption band was observed, because the exposed dye, which almost faded, contained a considerable amount of reaction intermediates before the dediazotization.

3.5.3. The reaction modes of azo dyes derived from 8N-acetyl-2-phenylazo-H-acid

Two dyes, Red BR and Red VSK, belong to this group. The values of $\Delta_f H^0$(gas) and $\Delta_f H^0$(H_2O) (cf. Table 2) indicate that Red BR and Red VSK exist as HTs in both the gas phase and water as well as on cellulose.

3.5.3.1. The HTs of Red BR. The values of d_{HOMO} listed in Table 6 suggest that the double bonds with possible reactivity toward $^1O_2$ are: C1=N11, C4=C5, C9=C10, C13=C14 and C13=C18. The $f^{(E)}_r$ values which give large $S^{(E)}_{m,n}$ values are listed in Table 3. The $\Delta_f H^0$(gas) values for the reaction intermediates and products at the corresponding double bonds are listed in Tables 8–10. The $\Delta_f H^0$(gas) values of the reaction products for the corresponding modes yield the following estimated order of reactivity:

Ene (C5=C4; H(N20)) may be excluded since hydrogen cannot be abstracted and the corresponding hydroperoxides cannot be formed. The double bonds C3=C8, C15=C16, C16=C17 may be excluded due to the small values of d_{HOMO} at C3 (0.000), C15 (0.004) and C17 (0.004). The reactivities estimated from the $S^{(E)}_{m,n}$ values seem to be consistent with order (5). At the double bond C1=N11, we concluded that mainly the ene reaction occurs, since we could not determine whether or not [2 + 2] addition contributes to the reactivity.

$$\begin{aligned}&\text{ene(C1=N11; H(N12))} > \text{[2 + 2]addition(C15=C16)}\\ &\approx \text{[2 + 2]addition(C9=C10)} > \text{[2 + 2]addition(C13=C14)}\\ &\approx \text{[2 + 2]addition(C13=C18)} > \text{[2 + 2]addition(C4=C5)}\\ &\approx \text{[2 + 2]addition(C16=C17)} > \text{[2 + 2]addition(C3=C8)}\\ &> \text{[2 + 2]addition(C1=N11).}\end{aligned} \quad (5)$$

The values of log k_0 were plotted on the ordinate, and the values of $S^{(E)}_{m,n}$ for the possible double bonds, listed in Table 2, were plotted on the abscissa one by one. The plot of $S^{(E)}_{m,n}$ (m, n: 1, 11; 4, 5; 18, 13, 14; 9, 10) against log k_0 showed a small deviation from the common correlation line in the direction of higher reactivity, as shown in Fig. 6. Whether or not the double bond C4=C5 contributed to the reactivity was difficult to determine. However, the plot of this dye did coincide with the common correlation line.

The values of $\Delta_f H^0$(gas) for the ATs of the reaction intermediates and products of each mode were also calculated (cf. Tables 8–10). They indicate that this dye undergoes AHT change during the reaction.

3.5.3.2. The HTs of Red VSK. The molecular geometry which deviated from the coplanar conformation showed higher stability than the coplanar conformation. The values of d_{HOMO}, listed in Table 6, yielded the following double bonds with possible reactivity against $^1O_2$: C1=N11, C13=C14, C13=C18, C16=C17 and C9=C10. The $f^{(E)}_r$ values giving large $S^{(E)}_{m,n}$ values are listed in Table 2. The relative ratio of the $f^{(E)}_r$ value to the d_{HOMO} at the corresponding positions varied widely. The contribution to the reactivity of a position with a d_{HOMO} value below the limiting value may be excluded, as mentioned above, even if the value of $f^{(E)}_r$ is high. When assessing the reactivity based on both the value of $f^{(E)}_r$ and d_{HOMO} at the same double bond, the lower limit of each value should be considered. Table 2 indicates that the double bonds C9=C10, C4=C5, C3=C8 and C1=N11 should be analyzed. The reactivities of the double bonds C4=C5 and C3=C8 may be excluded due to the small value of d_{HOMO} at C3 (0.000), C4 (0.000), C5 (0.004) and C8 (0.000), while those of the double

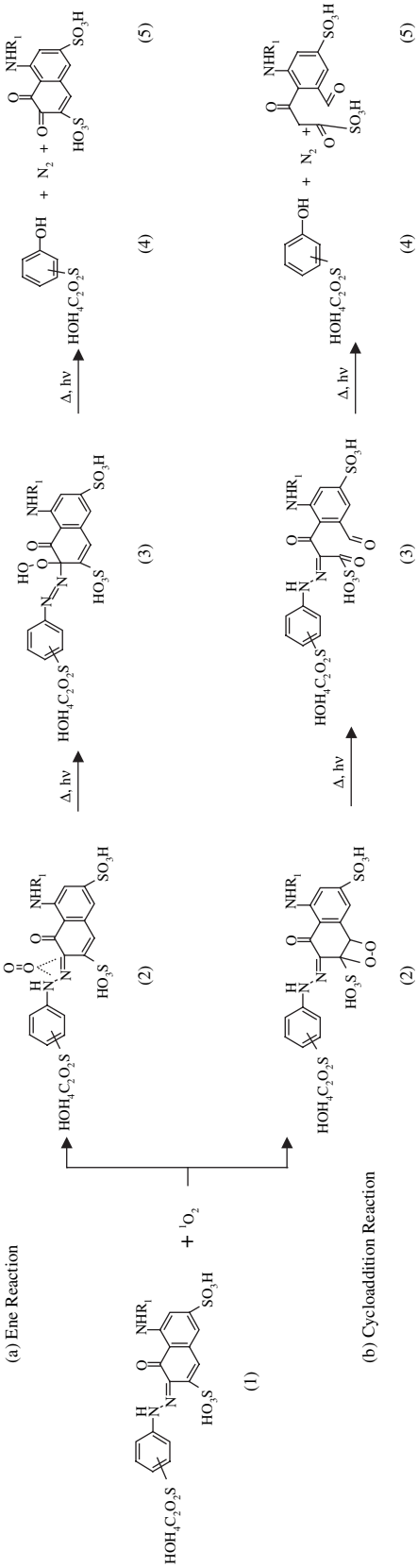

Scheme 1. (a) Ene (C1═N11; H(N12)) and (b) [2 + 2] cycloaddition (C9═C10) reactions of the HTs of a model phenylazo H-acid dye (1), which contains a vinylsulfonyl anchor in the diazo component, with singlet oxygen. In (a), (2): ene intermediate by the addition of singlet oxygen to the double bond at C1═N11, (3): the hydroperoxide via ene reaction, (4) and (5): thermal and/or photo-decomposed products from the hydroperoxide via dediazotization, where some by-products other than (4) and (5) may be formed. In (b), (2): 1,2-dioxetane via [2 + 2] cycloaddition (C9═C10) (the intermediate by the parallel addition of $^1O_2$ to the double bond of C9═C10 was omitted), (3): thermal and/or photo-decomposed products from the 1,2-dioxetanes, scission of C9═C10 bond, (4) and (5): thermal and/or photo-decomposed products from (3) via dediazotization, where some by-products other than (4) and (5) may be formed. (See text.).

Table 6
Electron densities, d_{HOMO}, at each atom for the A&HTs of Red BR and Red VSK in the gas phase, using PM5 method

	d_{HOMO}, Red BR[a]		d_{HOMO}, Red VSK[b]	
	AT	HT	AT	HT
C1	0.143	0.168	0.167	0.017
C2	0.124	0.008	0.108	0.000
C3	0.002	0.000	0.005	0.000
C4	0.103	0.026	0.035	0.000
C5	0.075	0.033	0.029	0.004
C6	0.028	0.001	0.009	0.000
C7	0.065	0.036	0.066	0.004
C8	0.000	0.010	0.014	0.000
C9	0.080	0.060	0.078	0.007
C10	0.032	0.044	0.002	0.007
N11	0.011	0.031	0.028	0.015
N12	0.046	0.254	0.051	0.022
C13	0.034	0.061	0.097	0.259
C14	0.018	0.041	0.040	0.070
C15	0.004	0.013	0.024	0.087
C16	0.036	0.075	0.048	0.134
C17	0.004	0.004	0.032	0.141
C18	0.019	0.052	0.016	0.012
O19	0.075	0.033	0.060	0.003
N20	0.062	0.016	0.027	0.001

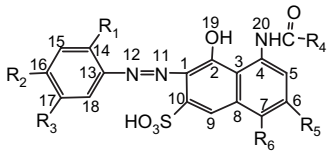

[a] Red BR ($R_1 = R_3 = R_6 = H$, $R_2 = m$-(2-hydroxyethylsulfonyl)anilinocarbonyl, $R_4 = CH_3$, $R_5 = SO_3H$).

[b] Red VSK ($R_1 = R_5 = H$, $R_2 = OCH_3$, $R_3 = 2$-hydroxyethylsulfonyl, $R_4 = CH_3$, $R_6 = SO_3H$).

bonds C9═C10 and C1═N11 are debatable. The values of d_{HOMO} at C9 and C10 were 0.007, which may also be a negligible value, compared with the values of d_{HOMO} at highly reactive positions: C13 (0.259), C14 (0.070), C15 (0.087), C16 (0.134) and C17 (0.141). Although the values of $f_r^{(E)}$ at C1 and N11 were quite large, the same situation seems to hold, since the values of d_{HOMO} are 0.017 at C1 and 0.015 at N11. Because the value of d_{HOMO} was 0.012 at C18, the contribution of this position may be excluded from the reactivity. The three double bonds C13═C14, C15═C16 and C16═C17 have very large $f_r^{(E)}$ and d_{HOMO} values compared with those of the other potential double bonds. Only these bonds can be said to contribute to the reactivity.

The $\Delta_f H^0$(gas) values of the reaction intermediates and products at the corresponding double bonds are listed in Tables 8–10. Based on the $\Delta_f H^0$(gas) values of the reaction products for the corresponding modes, the order of reactivity is as follows:

$$\begin{aligned}&\text{ene(C1═N11;H(N12))} \gg [2+2]\text{addition(C9═C10)}\\ &> [2+2]\text{addition(C15═C16)} > [2+2]\text{addition(C13═C18)}\\ &\approx [2+2]\text{addition(C4═C5)} \approx [2+2]\text{addition(C13═C14)}\\ &> [2+2]\text{addition(C3═C8)} > [2+2]\text{addition(C16═C17)}\\ &> [2+2]\text{addition(C1═N11)} \approx [2+2]\text{addition(C6═C7).}\end{aligned} \quad (6)$$

Order (6) did not coincide with the order yielded by the $S^{(E)}_{m,n}$ values, probably because of the inevitable structural change occurring during the formation of the intermediates and products. Except for the ene reaction, the $\Delta_f H^0$(gas) values of the reaction intermediates were in a narrow range, indicating no difference in the activation energy.

The plot of $S^{(E)}_{m,n}$ $(m, n$: 13, 14; 15, 16, 17) against $\log k_0$ coincided with the common correlation line of the series of dyes examined in this study, if the plots of the other dyes are added, as illustrated in Fig. 6.

3.5.3.3. The reaction scheme and the absorption spectra of the decomposed products. Although both Red BR and Red VSK exist as HTs in the gas phase and water, the preferential positions of reaction seem to be partially different: the position for Red BR seem to be C1═N11 followed by C18═C13, C13═C14, C9═C10 and C4═C5, while that for Red VSK seems to be C16═C17 followed by C16═C15 and C13═C14. Three of the reaction schemes are explained in Schemes 1(a), (b) and 2. The reactions in Red BR may occur preferentially on both sides of the atomic positions of the azo group. These reactions may result in the splitting off of the azo group as l,4-(3-(2-hydroxyethylsulfonyl)phenyliminocarbonyl)phenol, or as a related compound. The contribution of the reactions at C9═C10 and C4═C5, which may result in the ring opening of the naphthalene nucleus, may be small, because the absorption spectra of the decomposed products in the UV region exhibited some pattern changes with time (Fig. 2(a)). However, we inspected the time course of the spectra in detail during the exposure, and the visible spectra decreased monotonously, indicating the continuous decomposition of the chromophore through a primary photochemical reaction, whereas the absorption of the exposed sample near 200 nm increased in the beginning and then decreased, implying a stepwise decomposition of the intermediates generated by the primary reaction through reactions such as dediazotization. The spectra of the decomposed products between the wavelengths of 240 and 310 nm showed a time-dependent pattern accompanied by structural variations when the spectrum of the original dye at the corresponding concentration was subtracted (Fig. 2(a), spectra 6 and 7).

On the other hand, the preferred reaction mode for Red VSK may be the splitting off of the VS groups as a consequence of the formation of carbonyl groups at C16, followed by splitting off of the azo group. In the case of Red VSK, a mixture of at least two decomposed products seemed to be generated. As a result, the absorption spectra of the decomposed products of Red VSK seemed to resemble the spectral pattern of the decomposed products of Red BR, which have an *m*-VS-type anchor in common with the former [27] (cf. Fig. 2(b)). The spectra for Red VSK were simpler than those for Red BR and showed a monotonous increase of formation (cf. (Fig. 2(b), spectra 5 and 6), as the pattern did not vary with time.

The absorption spectra of the decomposed products and the exposed samples for the two dyes demonstrate that these reaction schemes are accurate.

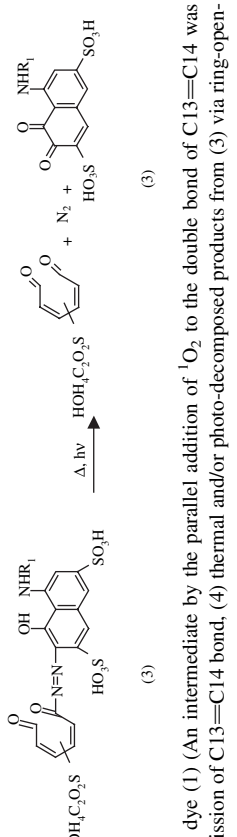

Scheme 2. [2 + 2] Cycloaddition (C13═C14) reaction of the ATs of a model VS-substituted phenylazo H-acid dye (1) (An intermediate by the parallel addition of $^1O_2$ to the double bond of C13═C14 was omitted), (2) 1,2-dioxetane generated, (3) thermal and/or photo-decomposed products from the 1,2-dioxetanes, scission of C13═C14 bond, (4) thermal and/or photo-decomposed products from (3) via ring-opening reaction, where some by-products other than (4) may be formed. (See text.).

3.5.4. The reaction modes of N-aroyl-2-phenylazo-H-acid dyes: C.I. Reactive Red 180 and Red VST

C.I. Reactive Red 180 belongs to this group. Red 180 is a typical VS dye with excellent light fastness. As explained below and in Section 3.5.5, the energy levels of the orbitals below HOMO seemed to vary considerably with the *N*-aroyl and *N*-aryl substituents.

3.5.4.1. The reactivity of the HTs of Red 180. This dye probably exists as HTs in the gas phase and water (cf. Table 2). Table 5 shows that the double bonds with possible reactivity against $^1O_2$ are C1═N11, C4═C5, C13═C22 and C16═C17. From the $\Delta_f H^0$(gas) values of the reaction intermediates and products listed in Tables 8–10, the order of reactivity for each mode can be estimated, as follows:

$$\begin{aligned}&\text{ene(C1═N11;H(N12))} > \text{[2 + 2]addition(C9═C10)}\\ &\approx \text{[2 + 2]addition(C4═C5)} > \text{[2 + 2]addition(C13═C22)}\\ &> \text{[2 + 2]addition(C17═C18)} > \text{[2 + 2]addition(C3═C8)}\\ &> \text{[2 + 2]addition(C1═N11).}\end{aligned} \tag{7}$$

This order is not consistent with the order given by the $S^{(E)}_{m,n}(m,n:)$ values (cf. Table 2). As with the other dyes, however, the plot of $S^{(E)}_{m,n}$ (m,n: 13, 22; 17, 18) against $\log k_0$ coincided fairly well with the common correlation line of the series of red dyes examined in this study (cf. Fig. 6). The double bond C4═C5 may manifest borderline reactivity due to the d_{HOMO} at C4 (0.014). According to the previous analyses [23–25], the $f^{(E)}_r$ value of 0.03 reflects the lower limit of reactivity, although we were not able to demonstrate this based on the absorption spectra of the decomposed products. But the $f^{(E)}_r$ values indicate that the reactivity of C1═N11 can be excluded (the $f^{(E)}_r$ values were used successfully to determine the reactivities of the other dyes). If some double bonds had $f^{(E)}_r \leq 0.03$ and others had $f^{(E)}_r \gg 0.3$, the former bonds would show no reactivity. This dye seems to possess two double bonds with high reactivity and many with borderline reactivity. If we take only the two double bonds with high reactivity into consideration, the plot of $S^{(E)}_{m,n}$ (m,n: 13, 22; 17, 18) against $\log k_0$ would show a good correlation with the other dyes. The reactive anchor of 1-sulfo-6-VS-2-naphtylamine lowered the $f^{(E)}_r$ values of the double bonds in the H-acid portion, resulting in low reactivity against $^1O_2$, but the connecting sites at C13 and C18 in the anchor group determined the reactivity.

3.5.4.1.1. The reaction scheme and the absorption spectra of the decomposed products. According to our analysis in terms of frontier orbital theory, the reactions with $^1O_2$ occurs in the diazo component, resulting in the formation of bis(carbonyl) fragments of the naphthalene ring at C13═C22 and in the splitting off of all chromophore parts at C18 as a result of [2 + 2] addition (C17═C18) (reaction schemes not shown).

The characteristic features of the absorption spectra of the decomposed products were a monotonous decrease of the visible band and an initial increase followed by a decrease of the absorption band at 230 nm with progressive fading with exposure (Fig. 3(a)); the spectral pattern itself was simple and showed no variation with exposure. This may indicate the stepwise decomposition of the reaction intermediates, such as the splitting off of the chromophore fragments through dediazotization. The characteristic pattern of the spectra in the UV region may demonstrate the reaction mechanism: the naphthalene ring opens and the naphthalene nucleus is split off, implying only the existence of VS anchor fragments and naphthalene ring fragments connected with the VS anchor.

3.5.4.2. The reactivity of the ATs of Red VST. This dye exists predominantly as ATs in both the gas phase and water. The double bonds with possible reactivity against $^1O_2$ are C1═C2, C4═C5, C17═C18, C13═C22, C9═C10, and C6═C7 (cf. Table 5). Besides the double bonds in the chromophore, our MO calculation showed that the double bonds in the phenyl group of the VS anchor group have considerable reactivity. From the values of $\Delta_f H^0$(gas) for the reaction intermediates and products at the corresponding double bonds, the following order of reactivity for each mode can be estimated (cf. Tables 8–10):

$$\begin{aligned}&\text{ene(C1═C2;H(O23))} \gg \text{ene(C5═C4;H(N24))}\\ &> \text{[2 + 2]addition(C4═C5)} \approx \text{[2 + 2]addition(C1═C2)}\\ &> \text{[2+2]addition(C17═C18)} > \text{[2+2]addition(C27═C32)}\\ &> \text{[2 + 2]addition(C9═C10)} > \text{[2 + 2]addition(C13═C22)}\\ &> \text{[2+2]addition(C28═C29)} > \text{[2+2]addition(C30═C31)}\\ &> \text{[2 + 2]addition(C6═C7)}\\ &\gg \text{[2 + 2]addition(N11═N12).}\end{aligned} \tag{8}$$

The double bonds C17═C18 and C13═C22 may contribute to the reactivity due to the large $f^{(E)}_r$ values, despite the small d_{HOMO} values. The reactivity at C6═C7 may be excluded due to the small $f^{(E)}_r$ value at C6, as with the other dyes. The order given by the $S^{(E)}_{m,n}$ values coincides fairly well with order (8).

The plot of $S^{(E)}_{m,n}$ (m,n: 1, 2; 4, 5; 27, 28; 29, 30; 31, 32) against $\log k_0$ resulted in a good agreement with the common correlation line, as illustrated in Fig. 6.

3.5.4.2.1. The reaction scheme and the absorption spectra of the decomposed products. According to above discussion, this tautomer may be decomposed via ene and [2 + 2] addition at C1═C2 and C5═C4 as well as at the double bonds in the phenyl group to which the VS anchor is attached. The reaction scheme for C1═C2 is shown in Scheme 1(a), although the dye structure should be modified. The reaction schemes for the [2 + 2] addition at C5═C4 and at the other double bonds (cf. Tables 2 and 4) are not given, but can be obtained by simply modifying the dye structures. The former reaction splits off the diazo component, while the latter at the double bonds in the phenyl group splits off the chromophore. The [2 + 2] addition of $^1O_2$ to the phenyl group

results in the generation of a phenyl group fragment or aliphatic groups without chromophores which are bound with the VS group. The absorption spectra of the decomposed products, illustrated in Fig. 3(b), were simple at wavelengths above 250 nm and different from those of *N*-aroyl-H-acid dyes, indicating reaction mechanisms characteristic of this dye. The calculated spectra showed a time-dependent pattern in the UV region below 250 nm at the beginning of exposure, implying the decomposition of the phenyl groups in the anchor. Although the relative amounts of end products without chromophores cannot be estimated, the spectra suggest the formation of more than two kinds of end products.

3.5.5. The reaction modes of 8N-(4-substituted triazinyl)-2-phenylazo-H-acid

3.5.5.1. The reaction modes of C.I. Reactive Red 194. The values of $\Delta_f H^0$(gas) suggest that this dye exists as ATs in the gas phase and as HTs in water (cf. Table 3). The reactivities of the ATs and HTs are analyzed next.

3.5.5.1.1. The ATs of Red 194. The d_{HOMO} values listed in Table 7 indicate that the double bonds with high possible reactivity toward $^1O_2$ are C1═C2, C3═C8, C4═C5, C6═C7, C9═C10, C13═C14, C13═C18, C15═C16, and N11═N12. The order of reactivity for each mode may be estimated from the values of $\Delta_f H^0$(gas) for the reaction intermediates and products at the corresponding double bonds, listed in Tables 8–10, as follows:

$$\begin{aligned}&\text{ene(C1═C2; H(O19))} > \text{[2 + 2]addition(C1═C2)}\\ &> \text{[2 + 2]addition(C4═C5)} > \text{[2 + 2]addition(C9═C10)}\\ &> \text{[2+2]addition(C13═C18)} > \text{[2+2]addition(C15═C16)}\\ &> \text{[2 + 2]addition(C6═C7)} > \text{[2 + 2]addition(C13═C14)}\\ &> \text{[2 + 2]addition(N11═N12)} > \text{[2 + 2]addition(C3═C8).}\end{aligned} \tag{9}$$

Although this dye possesses many double bonds with potential reactivity, the values of d_{HOMO} at C13 (0.018) and at C18 (0.022) may be at the boundary between reactivity and non-reactivity, while that at C14 (0.007) falls far below this boundary. Those at C6 (0.023) and at C7 (0.065) may also be at the boundary. The reactivities of the double bonds C3═C8, C13═C14, C15═C16, C16═C17 and N11═N12 can be excluded due to the small values of d_{HOMO} at C3 (0.004), C14 (0.007), C15 (0.010), C17 (0.000) and N11 (0.004).

The order of reactivity derived from the $S^{(E)}_{m,n}$ values for these double bonds seems to be similar to order (9). The plot of $S^{(E)}_{m,n}$ (m, n: 1, 2; 4, 5; 9, 10; 13, 18) against $\log k_0$ deviated considerably in the direction of higher reactivity (cf. Fig. 6). Here, the contribution of C6═C7 was ignored. Whether the double bond C6═C7 contributes to the reactivity or not could not be determined by this analysis, nor by the spectral analysis described below.

3.5.5.1.2. The HTs of Red 194. This tautomer showed a peculiar distribution of d_{HOMO}: very low values in the chromophore and high values in and around the triazine ring (cf. Table 7). This distribution resulted in low reactivity. In comparing the distribution of d_{HOMO} for the series of azo dyes derived from H-acids examined here, the very tenuous distribution of d_{HOMO} in the chromophore part may be observed in the HTs of Red 194, Red 227 and Red 4 and in the intermediary tautomer state of Red VST and Red 241, although no explanation for this was found.

The d_{HOMO} values in Table 7 suggest that the double bonds C1═N11, C4═C5, C6═C7, C9═C10, C13═C14 and C13═C18, which in the other dyes exhibit high possible reactivities toward $^1O_2$, possess no d_{HOMO}. From the values of $\Delta_f H^0$(gas) for the reaction intermediates and products at the corresponding double bonds, listed in Table 3, the following order of reactivity (cf. Tables 8–10) can be extracted:

$$\begin{aligned}&\text{[2 + 2]addition(C28═C29)} > \text{[2 + 2]addition(C32═C33)}\\ &> \text{[2 + 2]addition(C3═C8)} > \text{[2 + 2]addition(C30═C31).}\end{aligned} \tag{10}$$

The biased distribution of d_{HOMO} resulted in the low reactivity of this tautomer. The order of reactivity estimated based on the $S^{(E)}_{m,n}$ values for these double bonds seems to be different from order (10). Since the addition of $^1O_2$ may result in the modification in the geometry of the dyes, no accordance between them can be expected. The reactivity at C3═C8 may be excluded due to the low value of d_{HOMO} (0.000) at C8. The plot of $S^{(E)}_{m,n}$ (m, n: 28, 29, 30, 31, 32, 33) against $\log k_0$ deviated slightly in the direction of lower reactivity, as illustrated in Fig. 6. If both tautomers contribute to the reactivity, the value of k_0 against $^1O_2$ can be explained qualitatively. This indicates that Red 194 exists on cellulose as a mixture of ATs and HTs. The reaction scheme and absorption spectra of the decomposed products for this dye are discussed in Section 3.5.5.2.3 together with those of Red 227.

3.5.5.2. The reaction modes of Red 227. The values of $\Delta_f H^0$(gas) suggest that this dye exists as ATs in the gas phase and as HTs in water (cf. Table 3).

3.5.5.2.1. The ATs of Red 227. The double bonds of this dye with potential reactivity against $^1O_2$ may be similar to those of Red 194. Based on the values of $\Delta_f H^0$(gas) for the reaction intermediates and products, the order of reactivity (cf. Tables 8–10) is as follows:

$$\begin{aligned}&\text{ene(C1═C2; H(O19))} > \text{[2 + 2]addition(C1═C2)}\\ &> \text{[2 + 2]addition(C4═C5)} > \text{[2 + 2]addition(C9═C10)}\\ &> \text{[2+ 2]addition(C13═C18)} > \text{[2+2]addition(C15═C16)}\\ &> \text{[2 + 2]addition(C6═C7)} > \text{[2 + 2]addition(C13═C14)}\\ &> \text{[2 + 2]addition(C3═C8)} > \text{[2 + 2]addition(N11═N12).}\end{aligned} \tag{11}$$

Order (11) is almost identical to order (10). The order of reactivity yielded by the $S^{(E)}_{m,n}$ values almost coincide with order (11). As in the case of Red 194, the reactivities at C3═C8 and C13═C14 may be excluded due to the low

Table 7
Electron densities, d_{HOMO}, at each atom for the A&HTs of C.I. Reactive Red 194 and its related compounds in the gas phase, using PM5 method

Tautomer	Red 194[a]		Red 227[b]		Red 198[c]		Tautomer	Red 241[d]	
	AT, d_{HOMO}	HT, d_{HOMO}[e]	AT, d_{HOMO}	HT, d_{HOMO}[e]	AT, d_{HOMO}	HT, d_{HOMO}		AT, d_{HOMO}	HT, d_{HOMO}
C1	0.147	0.001	0.142	0.000	0.164	0.200	C1	0.130	0.114
C2	0.124	0.000	0.122	0.000	0.139	0.013	C2	0.111	0.003
C3	0.004	0.015	0.005	0.006	0.002	0.002	C3	0.004	0.001
C4	0.110	0.028	0.109	0.010	0.099	0.021	C4	0.121	0.034
C5	0.073	0.000	0.074	0.010	0.060	0.025	C5	0.081	0.043
C6	0.023	0.030	0.024	0.000	0.026	0.001	C6	0.023	0.000
C7	0.065	0.016	0.063	0.011	0.055	0.027	C7	0.073	0.047
C8	0.000	0.000	0.000	0.000	0.000	0.006	C8	0.002	0.023
C9	0.083	0.008	0.078	0.000	0.092	0.067	C9	0.079	0.045
C10	0.038	0.029	0.033	0.002	0.036	0.037	C10	0.047	0.055
N11	0.004	0.003	0.005	0.001	0.010	0.018	N11	0.001	0.042
N12	0.045	0.000	0.043	0.000	0.056	0.265	N12	0.039	0.218
C13	0.018	0.000	0.022	0.000	0.025	0.042	C13	0.007	0.025
C14	0.007	0.000	0.008	0.000	0.019	0.062	C14	0.004	0.035
C15	0.010	0.000	0.012	0.000	0.001	0.001	C15	0.000	0.000
C16	0.023	0.000	0.027	0.000	0.032	0.084	C16	0.010	0.054
C17	0.000	0.000	0.000	0.000	0.001	0.003	C17	0.000	0.001
C18	0.022	0.000	0.025	0.000	0.020	0.056	C18	0.005	0.032
O19	0.077	0.000	0.073	0.000	0.093	0.045	C19	0.001	0.013
N20	0.071	0.086	0.079	0.000	0.034	0.009	C20	0.001	0.006
C21	0.010	0.002	0.010	0.000	0.009	0.001	C21	0.008	0.046
N22	0.011	0.003	0.012	0.027	0.004	0.001	C22	0.008	0.048
C23	0.000	0.011	0.000	0.001	0.000	0.000	O23	0.068	0.016
N24	0.010	0.112	0.010	0.026	0.003	0.000	N24	0.089	0.042
C25	0.001	0.000	0.000	0.009	0.000	0.000	C25	0.010	0.002
N26	0.013	0.112	0.015	0.119	0.007	0.001	N26	0.012	0.003
N27	0.000	0.188	0.000	0.292	0.001	0.000	C27	0.000	0.000
C28	0.000	0.104	0.000	0.093	0.000	0.000	N28	0.009	0.002
C29	0.000	0.077	0.000	0.064	0.000	0.000	C29	0.000	0.000
C30	0.000	0.008	0.000	0.016	0.000	0.000	N30	0.025	0.016
C31	0.000	0.089	0.000	0.142	0.000	0.000	N31	0.005	0.005
C32	0.000	0.035	0.000	0.000	0.000	0.000			
C33	0.000	0.033	0.000	0.106	0.000	0.000			

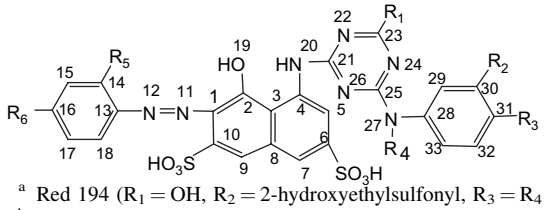

[a] Red 194 (R_1 = OH, R_2 = 2-hydroxyethylsulfonyl, $R_3 = R_4 = R_6$ = H, $R_5 = SO_3H$).
[b] Red 227 (R_1 = OH, $R_2 = R_4 = R_6$ = H, R_3 = 2-hydroxyethylsulfonyl, $R_5 = SO_3H$).
[c] Red 198 (R_1 = OH, $R_2 = SO_3H$, $R_3 = R_4 = R_5$= H, R_6 = 2-hydroxyethylsulfonyl).

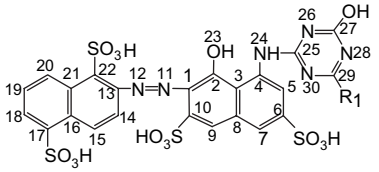

[d] Red 241 (R_1 = *p*-(2-hydroxyethylsulfonyl)phenylamino) (amino N = N31).
[e] The other d_{HOMO}'s exist in triazine and phenyl rings bound with VS group.

values of d_{HOMO} at C3 (0.005), C8 (0.000) and C14 (0.008). The double bonds C6═C7 and C15═C16 may contribute to the reactivity, in contrast to the analogous double bonds of Red 194, resulting in a higher reactivity than that of the ATs of Red 194.

As expected, the plot of $S^{(E)}_{m,n}$ (m, n: 1, 2; 4, 5; 6, 7; 9, 10; 13, 18; 15, 16) against $\log k_0$ showed a very large shift in the direction of higher reactivity from the common correlation line (cf. Fig. 6).

3.5.5.2.2. The HTs of Red 227. As in the case of the ATs, the d_{HOMO} seemed to be concentrated within the phenyl ring bound with the VS anchor. The lack of d_{HOMO} in the chromophore part was also observed in this tautomer. Based on the values of $\Delta_f H^0$(gas) for the reaction intermediates and

Table 8
Heat of formation, $\Delta_f H^0$(gas) (kcal mol^{-1}), of intermediate and products in the ene and [2 + 2] cycloaddition reactions at the double bonds of (C1═C2), (C1═N11), (C5═C4), C3═C8, etc. for the predominant tautomers of azo dyes derived from H-acid with singlet oxygen

Dye		Molecular weight	$\Delta_f H^0$(gas) of intermediate at TSG	$\Delta_f H^0$(gas) of intermediate	$\Delta_f H^0$(gas) of hydroperoxide	$\Delta_f H^0$(gas) of intermediate at TSG	$\Delta_f H^0$(gas) of intermediate	$\Delta_f H^0$(gas) of addition product
Mode (position)			Ene (C1═C2; H(O19))			[2 + 2] Addition (C1═C2)		
Red 194	AT	829.756	−352.937	−352.937	−407.065	−362.932	−362.779	−392.899
Red 227	AT	829.756	−358.667	−358.548	−408.801	−370.412	−370.409	−403.430
Red VSK	AT	635.589	−339.882	−339.882	−395.236	−34.714	−345.701	−380.244
Red VSP	AT	563.525	−269.786	−269.778	−317.732	−268.065	−268.040	−301.102
Congo VS	AT	467.468	−111.163	−110.997	−137.742	−111.168	−111.165	−130.212
Mode (position)			Ene (C1═C2; H(O23))			[2 + 2] Addition (C1═C2)		
Red 180	AT	797.751	−373.553	−373.553	−423.489	−381.622	−381.721	−412.787
Red 241	AT	959.874	−459.066	−458.996	−508.940	−458.152	−458.151	−488.685
Red VST	AT	812.766	−381.501	−381.501	−433.714	−388.558	−388.553	−415.653
Mode (position)			Ene (C1═N11; H(N12))			[2 + 2] Addition (C1═N11)		
Red 180	HT	797.751	−383.749	−383.714	−426.850	−383.748	−383.748	−387.755
Red 194	HT	829.756	−365.587	−365.587	−409.476[a]	−364.172	−364.214	−364.803
Red 198	HT	829.756	−365.435	−365.427	−408.456	−365.578	−365.569	−368.431
Red 227	HT	829.756	−367.964	−367.940	−415.300[a]	−369.540	−369.537	−371.035
Red 241	HT	959.874	−455.775	−455.768	−498.993	−457.673	−457.664	−467.104
Red BR	HT	724.685	−329.453	−330.582	−374.747	−331.483	−331.472	−333.184
Red VSK	HT	635.589	−351.382	−351.373	−397.193	−351.259	−351.254	−357.236
Red VSP	HT	563.525	−273.681	−273.673	−313.695	−271.799	−271.776	−278.097
			Ene (C5═C4; H(N24))			[2 + 2] Addition (C27═C32)		
Red VST	AT	812.766	−387.790	−387.761	−426.625	−387.639	−387.636	−410.502

Dye	Molecular weight	$\Delta_f H^0$(gas) of intermediate at TSG	$\Delta_f H^0$(gas) of intermediate	$\Delta_f H^0$(gas) of addition product	$\Delta_f H^0$(gas) of intermediate at TSG	$\Delta_f H^0$(gas) of intermediate	$\Delta_f H^0$(gas) of addition product
		[2 + 2] Addition (C3═C8) for AT			[2 + 2] Addition (C3═C8) for HT		
Red 180	797.751	–	–	–	−382.463	−382.461	−392.575
Red 194	829.756	−360.079	−360.072	−343.821	−362.921	−362.911	−374.656
Red 198	829.756	−363.692	−363.690	−365.216	−363.824	−363.819	−371.048
Red 227	829.756	−369.683	−369.690	−372.541	−369.883	−369.882	−373.312
Red 241	959.874	−458.761	−458.749	−460.961	−461.085	−461.085	−466.730
Red VST	812.766	−388.365	−388.363	−369.802	–	–	–
Red BR	724.685	–	–	–	−330.692	−330.692	−338.735
Red VSK	635.589	−345.633	−345.565	−355.219	−348.818	−348.788	−364.785
Red VSP	563.525	–	–	–	−271.557	−271.548	−278.822
Congo VS	467.468	−111.191	−111.185	−123.754	–	–	–
		[2 + 2] Addition (C16═C21) for AT			[2 + 2] Addition (C16═C21) for HT		
Red 241	959.874	−458.492	−458.492	−467.544	−459.806	−459.798	−473.541

[a] ATs.

products, listed in Table 3, the order of reactivity (cf. Tables 8–10) can be estimated as follows:

$$[2 + 2]\text{addition(C28═C29)} \approx [2 + 2]\text{addition(C28═C33)} > [2 + 2]\text{addition(C30═C31)}. \quad (12)$$

The distribution of d_{HOMO} in this tautomer may be more dispersed than in the HTs of Red 194, resulting in a lower reactivity than that of the HTs of Red 194. The reactivity at C32 may be excluded due to the very small value of d_{HOMO} at C32. The plot of $S^{(\mathrm{E})}_{m,n}$ (m, n: 33, 28, 29, 30, 31) against $\log k_0$ showed a considerable shift in the direction of lower reactivity from the common correlation line (Fig. 6).

As the AHT estimated by the MO calculation shows, this dye exists on cellulose substrate as a mixture of ATs and HTs, tautomers with completely different reactivities. The ATs of this dye have very high reactivity, much higher than of the ATs of Red 194, while the HTs have very low reactivity, much lower than of the HTs of Red 194. If the contribution to the reactivity of both tautomers is taken into consideration, the reactivity of Red 227 can be explained qualitatively.

3.5.5.2.3. The reaction scheme and the absorption spectra of the decomposed products of Red 194 and Red 227. As illustrated in Fig. 4(a) and (b), only slight differences were noticed in the absorption spectra in the visible region for the two dyes, while definite differences were found in the UV spectra: $\lambda_{\max}$ was near 290 nm and the two peaks were at 290 and 200 nm. Red 194 showed a strong peak at 287 nm, but it was lower than the peak at 200 nm, whereas Red 227 showed a strong peak at 290 nm, and it was larger than the peak at 200 nm. These differences can be used to distinguish these two dyes. The UV spectra of the decomposed products indicate that these differences were due to the effects of the geometry of

Table 9
Heat of formation, $\Delta_f H^0$(gas) (kcal mol^{-1}), of intermediates and products in the [2 + 2] additions at the double bonds of (C4=C5), (C6=C7), (C9=C10), (N11=N12) and (C32=C33)

Dye	Molecular weight	$\Delta_f H^0$(gas) of intermediate at TSG	$\Delta_f H^0$(gas) of intermediate	$\Delta_f H^0$(gas) of addition product	$\Delta_f H^0$(gas) of intermediate at TSG	$\Delta_f H^0$(gas) of intermediate	$\Delta_f H^0$(gas) of addition product
		[2 + 2] Addition (C4=C5) for AT			[2 + 2] Addition (C4=C5) for HT		
Red 180	797.751	−384.104	−384.103	−409.027	−384.320	−384.316	−404.091
Red 194	829.756	−365.422	−365.420	−390.261	−362.954	−362.953	−380.922
Red 198	829.756	−363.562	−363.561	−388.448	−363.574	−363.520	−384.694
Red 227	829.756	−371.215	−371.210	−396.066	−368.800	−368.811	−393.603
Red 241	959.874	−458.561	−458.513	−483.297	−452.503	−452.510	−473.968
Red VST	812.766	−375.068	−375.066	−415.968	−380.220	−380.206	−398.932
Red BR	724.685	−329.737	−329.732	−354.272	−331.931	−331.923	−348.302
Red VSK	635.589	−345.540	−345.197	−372.255	−349.217	−349.080	−368.252
Red VSP	563.525	−267.717	−267.591	−297.573	−271.552	−271.547	−294.596
Congo VS	467.468	−111.283	−111.276	−136.876	−99.692	−99.692	−119.327
		[2 + 2] Addition (C6=C7) for AT			[2 + 2] Addition (C6=C7) for HT		
Red 194	829.756	−368.040	−368.001	−374.530	−365.656	−365.653	−370.046
Red 198	829.756	−362.006	−362.002	−375.925	−362.788	−362.781	−372.969
Red 227	829.756	−370.088	−370.070	−380.277	−368.729	−368.727	−375.096
Red 241	959.874	−459.647	−459.611	−467.985	−582.587	−452.575	−467.316
Red VST	812.766	−375.034	−375.022	−388.782	−380.316	−380.309	−380.900
Red BR	724.685	−328.772	−328.768	−338.640	−331.819	−331.814	−335.519
Red VSK	635.589	−345.739	−345.674	−359.105	−348.781	−348.775	−357.142
Red VSP	563.525	−267.709	−267.614	−280.912	−271.516	−271.473	−278.492
Congo VS	467.468	−111.184	−111.142	−134.246	−100.053	−100.051	−120.235
		[2 + 2] Addition (C9=C10) for AT			[2 + 2] Addition (C9=C10) for HT		
Red 180	797.751	−383.885	−383.878	−399.482	−383.922	−383.916	−404.948
Red 194	829.756	−361.221	−361.215	−382.843	−365.675	−365.664	−371.953
Red 198	829.756	−362.069	−362.021	−381.523	−363.856	−363.552	−390.526
Red 227	829.756	−369.792	−369.711	−389.585	−371.646	−371.642	−388.369
Red 241	959.874	−458.637	−458.637	−478.576	−452.979	−452.976	−480.256
Red VST	812.766	−389.487	−389.482	−408.684	−380.164	−380.161	−406.653
Red BR	724.685	−328.036	−328.033	−346.915	−330.782	−330.760	−357.424
Red VSK	635.589	−347.625	−347.616	−366.470	−351.568	−351.568	−375.964
Red VSP	563.525	−268.726	−268.725	−283.322	−271.478	−271.478	−298.394
		[2 + 2] Addition (N11=N12) for AT			[2 + 2] Addition (C32=C33) for HT		
Red 194	829.756	−361.219	−361.218	−344.723	−365.290	−365.287	−380.469
Red 227	829.756	−369.892	−369.867	−349.107	−367.986	−367.958	−388.099
Red 241	959.874	−460.208	−460.085	−435.578	–	–	–
Red VST	812.766	−387.184	−387.126	−332.608	–	–	–
Congo VS	467.468	−111.066	−111.064	−93.424	–	–	–

the substituent VS groups in the anchor groups or the effects of the position of the VS groups.

Except for the fine differences in the spectra, the two dyes showed common AHT behaviors and photo-oxidation reaction schemes. Despite the differences in the relative positions of $\log k_0$ for the ATs and HTs of the two dyes as given by the MO calculation, the agreement between the experimental and the theoretical results demonstrates the validity of MO theory. The calculated absorption spectra of the decomposed products suggest the splitting off and/or the ring opening of the naphthalene ring, and the contribution of the HTs for both dyes may imply the generation of a mixture of decomposed products from the ring opening of the vinylsulfonylphenyl groups. As in the case of Congo VS and Red VSP (Fig. 1), at the beginning of exposure, a small increase of the base line in the visible region and a tiny time-dependent variation in the UV region were observed as well as the gradual formation of the end products, as illustrated in spectra 5 and 6.

These results are consistent with the predicted reaction schemes mentioned above, although no detailed analysis was possible.

3.5.5.3. The reaction modes of Red 241. The values of $\Delta_f H^0$(gas) indicate that this dye exists as a mixture of ATs and HTs in the gas phase and as ATs in water (cf. Table 3). The reactions of the HTs and ATs against $^1O_2$ are examined next.

3.5.5.3.1. The ATs of Red 241. Table 7 indicates that the double bonds which have possible reactivity against $^1O_2$ are C1=C2, C3=C8, C6=C7, C13=C14, C13=C22, C16=C21 C17=C18 and N11=N12. The reactivity of the double bonds C3=C8, C13=C14, C15=C16, C16=C17, C16=C21 and N11=N12 may be excluded due to the small values of d_{HOMO} at C3 (0.004), C8 (0.002), C14 (0.004), C15 (0.000), C16 (0.010), C17 (0.000) and N11 (0.001).

By calculating the $\Delta_f H^0$(gas) values for the reaction intermediates and products from these bonds by the PM5

Table 10
Heat of formation, $\Delta_f H^0$(gas) (kcal mol^{-1}), of intermediates and products in the [2 + 2] additions at the double bonds of (C13═C14), (C13═C18), (C14═C15), (C15═C16), (C16═C17), (C17═C18), (C13═C22), (C28═C29) and, (C30═C31)

Dye	Molecular weight	$\Delta_f H^0$(gas) of intermediate at TSG	$\Delta_f H^0$(gas) of intermediate	$\Delta_f H^0$(gas) of addition product	$\Delta_f H^0$(gas) of intermediate at TSG	$\Delta_f H^0$(gas) of intermediate	$\Delta_f H^0$(gas) of addition product
		[2 + 2] Addition (C13═C14) for AT			[2 + 2] Addition (C13═C14) for HT		
Red 180	797.751	–	–	–	−382.427	−382.424	−394.876
Red 194	829.756	−362.699	−362.699	−372.279	−362.949	−362.942	−367.817
Red 198	829.756	−361.968	−361.965	−376.236	−363.605	−363.595	−382.089
Red 227	829.756	−356.565	−356.563	−377.100	−368.794	−368.787	−374.401
Red BR	724.685	−330.107	−330.106	−347.001	−331.931	−331.923	−350.547
Red VSK	635.589	−345.622	−345.603	−360.192	−348.329	−348.281	−367.769
Red VSP	563.525	−267.728	−267.724	−271.216	−271.220	−271.214	−289.552
Congo VS	457.468	−111.062	−110.061	−127.742	−100.312	−100.304	−118.550
		[2 + 2] Addition (C13═C18) for AT			[2 + 2] Addition (C13═C18) for HT		
Red 194	829.756	−367.447	−367.430	−378.856	−363.317	−363.309	−385.402
Red 198	829.756	−361.930	−361.927	−378.923	−363.582	−363.487	−378.912
Red 227	829.756	−369.002	−368.968	−388.593	−370.809	−370.804	−389.180
Red BR	724.685	−329.871	−329.863	−344.154	−331.826	−331.819	−350.245
Red VSK	635.589	−345.793	−345.767	−364.807	−348.293	−348.246	−369.014
Red VSP	563.525	−267.675	−267.611	−284.406	−271.227	−271.161	−289.564
		[2 + 2] Addition (C15═C16) for AT			[2 + 2] Addition (C15═C16) for HT		
Red 194	829.756	−366.690	−366.686	−377.660	−369.750	−369.696	−383.207
Red 227	829.756	−363.868	−363.867	−381.327	−363.819	−363.818	−386.972
Red BR	724.685	−329.923	−329.922	−346.510	−331.779	−331.778	−357.867
Red VSK	635.589	−345.688	−345.657	−368.906	−348.702	−348.676	−373.326
		[2 + 2] Addition (C14═C15) for AT			[2 + 2] Addition (C14═C15) for HT		
Red BR	724.685	–	–	–	−329.438	−329.438	−347.873
Red VSK	635.589	−345.683	−345.636	−364.570	−348.750	−348.725	−368.139
Red VSP	563.525	−267.605	−267.585	−283.262	−271.242	−271.217	−287.377
		[2 + 2] Addition (C16═C17) for AT			[2 + 2] Addition (C16═C17) for HT		
Red BR	724.685	−329.953	−329.879	−345.640	−329.438	−329.434	−347.873
Red VSK	635.589	−345.710	−345.691	−359.500	−351.104	−351.097	−362.660
		[2 + 2] Addition (C17═C18) for AT			[2 + 2] Addition (C17═C18) for HT		
Red 180	797.751	−384.003	−383.998	−396.349	−384.717	−384.706	−395.585
Red 241	959.874	−458.399	−458.394	−474.882	−457.080	−457.065	−473.666
Red VST	812.766	−387.537	−387.525	−414.591	−387.341	−387.338	−413.807
		[2 + 2] Addition (C13═C22) for AT			[2 + 2] Addition (C13═C22) for HT		
Red 180	797.751	−381.012	−381.009	−399.238	−383.756	−383.755	−401.106
Red 241	959.874	−460.460	−460.458	−476.076	−455.269	−455.202	−482.401
Red VST	812.766	−387.550	−387.549	−406.231	–	–	–
		[2 + 2] Addition (C28═C29) for HT			[2 + 2] Addition (C30═C31) for HT		
Red 194	829.756	−364.909	−364.842	−384.992	−363.804	−363.731	−373.691
Red 227	829.756	−367.910	−367.910	−381.901	−367.694	−367.691	−375.174
		[2 + 2] Addition (C28═C29) for AT			[2 + 2] Addition (C30═C31) for AT		
Red VST	812.766	−387.655	−387.637	−405.079	−387.538	−387.536	−396.378

method, the following order of reactivity can be established (cf. Tables 8–10):

$$\begin{aligned}&\text{ene(C1═C2; H(O23))} > \text{[2 + 2]addition(C1═C2)}\\ &> \text{[2 + 2]addition(C4═C5)} > \text{[2 + 2]addition(C9═C10)}\\ &> \text{[2 + 2]addition(C13═C22)} > \text{[2+2]addition(C17═C18)}\\ &> \text{[2 + 2]addition(C6═C7)} \approx \text{[2 + 2]addition(C16═C21)}\\ &> \text{[2 + 2]addition(N11═N12).}\end{aligned} \quad (13)$$

The contribution of the double bond N11═N12 to the reactivity may be excluded due to the very high energy barrier for forming the corresponding reaction products (cf. Table 10).

Order (13) does not coincide with the order given by the $S^{(E)}_{m,n}$ values. Thus, the plot of $S^{(E)}_{m,n}$ (m, n: 1, 2; 4, 5; 9, 10) against $\log k_0$ is in good agreement with the common correlation line (cf. Fig. 6).

3.5.5.3.2. The HTs of Red 241. As in the case of the ATs, the $\Delta_f H^0$(gas) values for the reaction intermediates and

products from the possible bonds can be used to determine the order of reactivity, as follows (cf. Tables 8–10):

$$\begin{aligned}&\text{ene(C1=N11;H(N12))} > \text{[2 + 2]addition(C13=C22)}\\ &> \text{[2 + 2]addition(C9=C10)} > \text{[2 + 2]addition(C4=C5)}\\ &\approx \text{[2 + 2]addition(C17=C18)} \approx \text{[2 + 2]addition(C16=C21)}\\ &> \text{[2 + 2]addition(C6=C7)} \approx \text{[2 + 2]addition(C1=N11)}\\ &\approx \text{[2 + 2]addition(C3=C8).}\end{aligned} \tag{14}$$

The order of reactivity yielded by the $S^{(E)}_{m,n}$ values does not coincide with order (14). The contribution of the double bond C3=C8 may be excluded due to the very small values of d_{HOMO} at C3 (0.001). In the HTs, many possible double bonds (Table 3) contribute to the reactivity, and the reactivity of the HTs is higher than that of the ATs.

The plot of $S^{(E)}_{m,n}$ (m,n: 1, 11; 16, 21; 9, 10; 14, 13, 22; 4, 5) against $\log k_0$ showed a small shift in the direction of higher reactivity from the common correlation line (cf. Fig. 6). If the contributions of both the ATs and the HTs to the reactivity are taken into consideration, the reactivity of Red 241 can be explained qualitatively.

3.5.5.3.3. The reaction scheme and the absorption spectra of the decomposed products of Red 241. As shown in Fig. 5(b), the absorption spectra of the decomposed products of Red 241 resemble those of the decomposed products of azobenzene dyes with a triazinyl anchor group [24] and the red dyes of this group derived from H-acid with bifunctional reactive groups, implying that the VS or the sulfo-anilinotriazinyl anchor group bound with cellulose may be the main end product; a mixture of related compounds may be the secondary products, which may indicate the splitting off and/or the ring opening of the naphthalene ring (the diazo component). Although not all reaction schemes are mentioned in this paper, the schemes mentioned above seem to be consistent with the spectra of the decomposed products, but detailed analysis of the reaction mechanisms was impossible.

3.5.6. The reaction modes of the HTs of Red 198

The values of $\Delta_f H^0$(gas) indicate that this dye exists as HTs in both the gas phase and in water (cf. Table 3). The $\Delta_f H^0$(gas) values for the reaction intermediates and products from the possible double bonds suggest the following order of reactivity:

$$\begin{aligned}&\text{ene(C1=N11;H(N12)} > \text{[2 + 2]addition(C9=C10)}\\ &> \text{[2 + 2]addition(C4=C5)}\\ &> \text{[2+2]addition(C13=C14)=[2+ 2]addition(C13=C18)}\\ &> \text{[2 + 2]addition(C6=C7)} > \text{[2 + 2]addition(C1=N11).}\end{aligned} \tag{15}$$

The order of reactivity given by the $S^{(E)}_{m,n}$ values does not coincide with order (15). The reactivities of the double bonds C1=N11, C3=C8, C4=C5 and C6=C7 can be excluded due to the small values of d_{HOMO} at N11 (0.018), C4 (0.021), C5 (0.025) and C7 (0.027), and due to the borderline value of $f_r^{(E)}$ at N11 (0.031). If, as in the case of Red 180 and its extensions, the three double bonds with $f_r^{(E)} \geq 0.07$ contribute to the reactivity and the double bonds with $f_r^{(E)} \leq 0.05$ do not, the present MO calculation yields a good correlation. Thus, the plot of $S^{(E)}_{m,n}$ (m,n: 9, 10; 14, 13, 18) against $\log k_0$ shows a good coincidence with the common correlation line, as shown in Fig. 6.

3.5.6.1. The reaction scheme and the absorption spectra of the decomposed products. The good coincidence of the plot of this dye with the common correlation line implies the validity of the present analysis using MO theory. Experimental verification based on the absorption spectra of the decomposed products may be in principle impossible due to the incomplete binding of the dye with cellulose. This dye has two reactive anchor groups in remote positions: a VS group in the diazo component and an MCT group in the coupling component. As illustrated in Fig. 5(a), the spectra suggest the absence of any superposition of more than two kinds of products. In the present study, Red 198 was dyed using the alkali-shock method (alkaline fixation after exhaustion under neutral conditions). Since about two anchor groups bind with cellulose, this dye showed a good coincidence with the common correlation line.

3.6. The general structure–property relationship of azo dyes derived from H-acid

H-acid is the intermediate most frequently used for the coupling component in reactive dyes. Naphthalene has many fixed double bonds, which cannot be shifted easily by substituents, with only a few exceptions. In the present study, MO theory could pinpoint only three exceptional dyes with low reactivity: C.I. Reactive Red 180, Red 198 and Red 241. We could not identify any principle by which one can synthesize azo dyes derived from H-acid with low reactivity against $^1O_2$, although we were able to analyze the reactivity of azo dyes derived from H-acid against $^1O_2$ by finding the common correlation line between $\log k_0$ and the sum of $f_r^{(E)}$ for the series of azo dyes derived from H-acid examined in this study.

In the previous papers, similar but different correlation lines, which lie in different positions in the co-ordinate system of $\log k_0$ and the sum of $f_r^{(E)}$ and have nearly the same slope, were found for a series of azo dyes derived from γ- and J-acids [25], from the pyrazoline ring [23] and for a series of azobenzene dyes [24] as well as for a series of dyes derived from H-acid examined in the present study, although this fact may indicate that the orbital energy differences between the HOMO of the dyes and the LUMO of the $^1O_2$ should be taken into consideration when estimating the reactivity; Fukui and Fujimoto have referred to this as superdelocalizability [29]. So, using an accurate common correlation line for a series of dyes with similar structures, one can create QSAR applications for the purpose of designing azo dyes with high photo-oxidation stability, just as in drug design [18–20]. When designing ideal azo dyes at the molecular level, one can use these correlation lines without synthesizing all of the model dyes or calculate the sum of $f_r^{(E)}$ using the PM5 method, although these methods may not produce good perspiration/light fastness. In

general, one can identify or create molecular structures with exceptional and/or extrapolated properties.

Together with the previous series of studies on monoazo reactive dyes, the present experimental and MO study on the reactivity of monoazo dyes against $^1O_2$ may be a breakthrough in the field of molecular dye design.

4. Summary

The reactivities of 10 monoazo reactive dyes derived from H-acid and related naphthalene sulfonic acids were experimentally determined by exposing dyed cellophane immersed in aerobic aqueous RB solution to a carbon arc. These dyes exhibited AHT, depending upon the solvation effect of the medium in which they existed. If a dye existed as the same tautomer in both the gas phase and water, it was assumed that the dye exists as the same tautomer on water-swollen cellulose. But if the dye existed as different tautomers in the gas phase and water, since we have no procedure to identify the tautomer on cellulose directly, we examined the reactivities of both tautomers. The AHT of the dyes on water-swollen cellulose was determined by calculating the $\Delta_f H^0$(gas) and $\Delta_f H^0(H_2O)$ values. The reactivity of the 10 dyes toward $^1O_2$ was quantum-mechanically estimated based on frontier electron theory or the sum of $f_r^{(E)}$ at the atomic positions of the double bonds which exceeded the d_{HOMO} limit, and the $f_r^{(E)}$ values were estimated by the PM5 method in the gas phase for the ATs and/or HTs of the corresponding dyes.

$^1O_2$ reacts with the double bonds in the dye molecule through the ene and/or the $[2+2]$ cycloaddition reaction, yielding hydroperoxide via 1,3-addition and/or dioxetane or carbonyl fragments, respectively. These reactions occur mainly at the atomic positions of the bridge roots. The reaction intermediates are further decomposed through reactions such as dediazotization. We were able to confirm the reaction mechanisms using the absorption spectra of the photo-decomposed products and spectral analysis.

The sum of $f_r^{(E)}$ against $\log k_0$ was plotted for each dye, and a good linear correlation line was found between the dyes. The correlation lines for the different series of azo dyes examined in this and in previous studies had similar slopes but different positions, implying that the difference between the energy levels of HOMO of the dyes and the LUMO of the $^1O_2$ may contribute to the reactivity, as Fukui explained in his theory of superdelocalizability.

Monoazo dyes derived from H-acid usually possess considerable reactivity against $^1O_2$ due to properties such as large d_{HOMO} values at the coupling position and fixed double bonds in the naphthalene ring. To date, no one can synthesize azo dyes derived from H-acid with excellent fastness against $^1O_2$.

Acknowledgement

This work was supported by a Grant-in-Aid for Scientific Research given by the Ministry of Education, Culture, Sports, Science and Technology, Japan.

References

[1] Griffiths J, Hawkins C. Oxidation by singlet oxygen of arylazonaphthols exhibiting azo–hydrazone tautomerism. Journal of the Chemical Society, Perkin Transactions 2 1977;6:747–52.
[2] Rembold MW, Kramer HEA. Singlet oxygen as an intermediate in the catalytic fading of dye mixtures. Journal of the Society of Dyers and Colourists 1978;94(1):12–7.
[3] Griffiths J, Hawkins C. Synthesis and photochemical stability of 1-phenylazo-2-naphthol dyes containing insulated singlet oxygen-quenching groups. Journal of Applied Chemistry and Biotechnology 1977;27:558–64.
[4] Lyčka A, Macháček V. ^{13}C- and ^{15}N NMR studies of the azo–hydrazone tautomerism of some azo dyes. Dyes and Pigments 1986;7(3):171–85.
[5] Mustroph H, Weiss C. Fading behavior of tautomerizable azo dyes. IV. Quantum-chemical calculations for the photofading mechanism of 1-phenylazo-naphthols. Zeitschrift für Chemie 1983;23(2):61–2.
[6] Mustroph H, Potocnak J, Grossmann N. Studies of the photochemical fading of tautomeric dyes. VI. Photochemical oxidation of phenylazoacetylacetones and phenylazopyrazolones by singlet oxygen. Journal für Praktische Chemie 1984;326(6):979–84.
[7] Mustroph H, Weiss C. Investigations of the photofading behavior of hydrazones. Journal für Praktische Chemie 1986;328(5–6):937–40.
[8] Morita Z, Hada S. A semiempirical molecular orbital study on the reaction of an aminopyrazolinyl azo dye with singlet molecular oxygen. Dyes and Pigments 1999;41(1):1–10.
[9] Hihara T, Okada Y, Morita Z. Reactivity of phenylazonaphthol sulfonates, their estimation by semiempirical molecular orbital PM5 method, and the relation between their reactivity and azo–hydrazone tautomerism. Dyes and Pigments 2003;59(3):201–22.
[10] Okada Y, Hirose M, Kato T, Motomura H, Morita Z. Photofading of vinylsulfonyl reactive dyes on cellulose under wet conditions. Dyes and Pigments 1990;14(2):113–27.
[11] Okada Y, Hirose M, Kato T, Motomura H, Morita Z. Fading of vinylsulfonyl reactive dyes on cellulose in admixture under wet conditions. Dyes and Pigments 1990;14:265–85.
[12] Okada Y, Motomura H, Morita Z. Photosensitization and simultaneous reductive or oxidative fading of monochlorotriazinyl reactive dyes on cellulose under wet conditions. Dyes and Pigments 1992;20(2):123–35.
[13] Okada Y, Hirose M, Kato T, Motomura H, Morita Z. Catalytic fading of vinylsulfonyl reactive dye mixtures on cellulose under wet conditions. Dyes and Pigments 1990;12(3):197–211.
[14] Okada Y, Morita Z. Fading of some vinylsulfonyl reactive dyes on cellulose under various conditions. Dyes and Pigments 1992;18(4):259–70.
[15] Okada Y, Motomura H, Morita Z. Simultaneous oxidative and reductive photofading of C.I. Reactive Red 22 and Black 5 on cellulose in presence of oxygen and substrate under wet conditions. Dyes and Pigments 1991;16(3):205–21.
[16] Okada Y, Orikasa K, Motomura H, Morita Z. Oxidative and reductive fading of monochlorotriazinyl reactive dyes on cellulose under wet conditions. Dyes and Pigments 1992;19(3):203–14.
[17] Okada Y, Kato T, Motomura H, Morita Z. Fading mechanism of reactive dyes on cellulose by simultaneous effects of light and perspiration. Sen'i Gakkaishi 1990;46(8):346–55.
[18] Kubinyi H. Quantitiative structure–activity relationships in drug design. In: Schleyer P von R, editor. Encyclopedia of computational chemistry, 4. Chichester: Wiley; 1998. p. 2309–20.
[19] Jurs PC. Quantitiative structure–property relationships (QSPR). In: Schleyer P von R, editor. Encyclopedia of computational chemistry, 4. Chichester: Wiley; 1998. p. 2320–30.
[20] Karelson M. Molecular descriptors in QSAR/QSPR. New York: Wiley-Interscience; 2000.
[21] Fabian J, Hartmann H. Light absorption of organic colorants, theoretical treatment and empirical rules. In: Reactivity and structure concepts in organic chemistry 12. Berlin: Springer-Verlag; 1980.
[22] Hihara T, Okada Y, Morita Z. Azo–hydrazone tautomerism of phenylazonaphthol sulfonates and their analysis using the semiempirical

molecular orbital PM5 method. Dyes and Pigments 2003;59(1): 25–41.
[23] Hihara T, Okada Y, Morita Z. Photo-oxidation of pyrazolinylazo dyes and analysis of reactivity as azo and hydrazone tautomers using semiempirical molecular orbital PM5 method. Dyes and Pigments 2006;69(2):151–76.
[24] Hihara T, Okada Y, Morita Z. The photo-oxidation of reactive azobenzene dyes and an analysis of their reactivity for the azo and hydrazone tautomers using semiempirical molecular orbital PM5 method. Dyes and Pigments 2007;75(1):225–45.
[25] Hihara T, Okada Y, Morita Z. A semiempirical molecular orbital study on the photo-reactivity of monoazo reactive dyes derived from γ- and J-acid. Dyes and Pigments 2007;73(2):141–61.
[26] Hihara T, Okada Y, Morita Z. Relationship between photochemical properties and colourfastness due to light-related effects on monoazo reactive dyes derived from H-acid, γ-acid, and related naphthalene sulfonic acids. Dyes and Pigments 2004;60(1):23–48.
[27] CAChe reference guide [CAChe reference guide 4.9; 3-9–3-10]. Fujitsu Ltd.;2005.
[28] Hihara T, Okada T, Morita Z. Photofading, photosensitization, and effect of aggregation on fading of triphenodioxazine and copper phthalocyanine dyes. Dyes and Pigments 2001;50(3):185–201.
[29] Fukui K, Fujimoto H, editors. Frontier orbitals and reaction paths, selected papers of Fukui K. World Scientific series in 20th century chemistry, vol. 7. Singapore: World Scientific; 1997.